S17 Theoretical and Particle Physics
Física Teórica y de Partículas (DFTP)

11/07 Monday afternoon, Aula 1.16 bis

15:30-15:45 Aniol Lobo Salvia
LHCb Commissioning for run 3 - Milestones in the Trigger System

15:45-16:00 Diego Mendoza Granada
Trigger challenges for detecting long-lived particles at LHCb

16:00-16:15 Carlos García Montoro
IFIC Contributions to the Computing of the ATLAS Experiment for the Run 3 of the LHC

16:15-16:30 Ángel Jesús Murcia Gil
Exact electromagnetic duality with nonminimal couplings

16:30-16:45 Rafael Delgado López
quantumfdtd, a computational framework for the Relativistic Schrödinger Equation

16:45-17:00 Adrián Casado Turrión
Is gravitational collapse possible in f(R) gravity?

17:00-18:00 **Posters and Coffee**

18:00-18:15 Shalini Epari
Search for flavourful 2HDM model in multilepton plus multi-b-jets final states

18:15-18:30 Mariam Chitishvili
Measurement of the quadruple-differential angular decay rates of single top quarks produced in the t-channel at ?s=13 TeV

18:30-18:45 Pablo Martínez-Agulló
Search for associated production of a Higgs boson and a single-top quark in the 2l+tau final state at 13 TeV in ATLAS

18:45-19:00 Pablo Martínez-Agulló
Search for associated production of a Higgs Boson and a single top quark in 3l and 2lSS final states at 13 TeV in ATLAS

19:00-19:15 Mariia Didenko
Search for long-lived neutral particles in pp collisions at 13 TeV that decay into displaced hadronic jets in the ATLAS calorimeter

Posters:

39 Laura Remón Martín
Electromagnetic tensor endowed with polarimetric parameters: application to the vicinity of extremely dense bodies

40 Víctor Montesinos Llácer
Prediction of symmetric partners of the Zc(3900) and Zb(10610) exotic states using heavy quark spin symmetry and SU(3) flavor symmetry

S17 Theoretical and Particle Physics
Física Teórica y de Partículas (DFTP)

12/07 Tuesday afternoon, Aula 1.16 bis

15:30-15:45 Carlos Solans Sanchez
Radiation hardness and timing performance of MALTA monolithic Pixel sensors in Tower 180 nm

15:45-16:00 Rafael Mayo García
Technological Applications of Extensive Air Showers Simulations

16:00-16:15 Paula Garcia Moreno
Commissioning and Monitoring of the Calorimeter sub-detector in LHCb experiment

16:15-16:30 Rodrigo Alvarez Garrote
Simulation and reconstruction of scintillation light with X-ARAPUCA photodetectors in SBND

16:30-16:45 Rafael Delgado López
Unitarized one-loop graviton-graviton scattering

16:45-17:00 Álvaro Parra López
Gravitational particle production in the laboratory

17:00-18:00 **Coffee Break**

18:00-18:15 Felipe J. Llanes-Estrada
Some uses of dispersion relations

18:15-18:30 Miguel Albaladejo Serrano
On the doubly charmed tetraquark Tcc+ recently discovered at CERN: analysis and predictions

18:30-18:45 César Jesús Valls
Analysis and instrumentation developments for the future understanding of neutrino physics with the T2K experiment

18:45-19:00 Paula Martinez Suarez
The ATLAS Level-1 Topological Trigger: Run 2 performance and plans for Run 3

S17 Theoretical and Particle Physics
Física Teórica y de Partículas (DFTP)

13/07 Wednesday afternoon, Aula 1.16 bis

15:30-15:45 Naseem Bouchhar
Data-Driven Calibration of B-Tagged and Large-R Jets for gamma+jet Events in The ATLAS Experiment

15:45-16:00 Héctor García Cabrera
Results of the SDHCAL Beam Test data analysis of 2015

16:00-16:15 Juan Ramón Balaguer Tornel
IIB orientifold reductions with open strings

16:15-16:30 Sergio Manthey Corchado
Light Detection in DUNE's Vertical Drift Module

16:30-16:45 Laura Pérez Molina
Photon Detection System in ProtoDUNE phase II

16:45-17:00 Pablo Barham Alzás
Core-Collapse Supernova Burst Neutrino detection and trigger in DUNE

17:00-18:00 **Coffee Break**

S17 Theoretical and Particle Physics
Física Teórica y de Partículas (DFTP)

14/07 Thursday afternoon, Aula 1.16 bis

15:30-16:30 Seminario: Guillelmo Ceballos (MIT)
La medida de la masa del W por el experimento CDF

16:30-17:00 Entrega de premios de tesis doctorales

17:00-18:00 **Coffee Break**

18:00-19:30 Junta de Gobierno de la DFTP

Two lines of space reserved to include
codes of the symposium and of this communication

LHCb Commissioning for run 3 Milestones in the Trigger System

Aniol Lobo Salvia

ICCUB, Martí i Franquès 1 Barcelona, Spain

e-mail: aniol.lobo.salvia@cern.ch

This talk aims to provide a brief description of the *Trigger System* of LHCb, its upgrades for run 3 and its particular implantation for the *Radiative Processes Subgrup* as a use case.

The LHCb detector is a single-arm spectrometer designed to provide competitive measurements of CP violation and rare decays of B hadrons [1]. Data taking occurs in campaigns of approximately four years called *runs* separated by *Long Shutdown* periods. The upgrades introduced in the trigger system during the Long Shutdown II will be here discussed.

The trigger system is the responsible of deciding when to store the result of a collision, what we call *event.* From the 30 million collisions that occur per second in the LHCb a large fraction of them are of poor interest. This occurs mainly because they either contain a process already measured with high precision or a collision with low momentum transfer, as opposed to the events containing b quarks which we centre our attention on. The trigger must provide a balance when saving decays interesting for different types of analysis, always keeping a bandwidth acceptable by the data acquisition system [DAQ] and the storage capacity.

The framework update for the trigger system has three main advantages

· Removal of the hardware-based trigger filter [L0]

· Having more information at the stage of the trigger decision

· Offering to possibility to store only the information of the event relevant to the posterior analysis

The first milestone has been achieved via the full optimization of the reconstruction and selection algorithms and via increasing the computing power of the farms, allowing all events to be processed by GPUs and CPUs.

The second milestone was also possible by the optimization of the reconstruction algorithms needed to transform raw detector signal to information relevant to the filtering of events according to physical properties of the reconstructed particles. This was previously done in two stages in the first and second runs due to its high computational cost.

The third major improvement allows for the storage of a larger number of events given a permitted bandwidth, since the weight of the part of the event stored is smaller than the whole event.

[1] LHCb Collaboration, A. A. Alves et al., The LHCb detector at the LHC, *Journal of Instrumentation* **3** (2008).

Trigger challenges for detecting long-lived particles at LHCb

Arantza Oyanguren Campos[1,*], **Diego Mendoza Granada**[2,*], Louis Henry[3,**]

[1]*oyangur@ific.uv.es* [2]*diego.mendoza.granada@cern.ch* [3]*louis.henry@cern.ch*

[*]*Experimental unit, Instituto de Física Corpuscular (IFIC). Carrer del Catedrátic José Beltrán Martinez, 2, 46980 Paterna, Valencia. Spain*

[**]*EP/LBD, CERN. Esplanade des Particules 1, 1217 Meyrin. Switzerland*

Collider experiments in high-energy physics (HEP) have sought to test the Standard Model of particle physics (SM), the most successful theory of fundamental interactions. Nonetheless, it is unable of explaining some empirically observed phenomena such as the imbalance of matter and antimatter in the Universe, neutrino masses or the origin of dark matter. This has therefore motivated New Physics (NP) extensions involving beyond the Standard Model (BSM) particles that may be observable in proton-proton collision experiments such as the Large Hadron Collider (LHC) at CERN. The interest in long-lived particles (LLPs) is growing in the HEP community, specially for high-luminosity LHC and B-factory experiments. One of the main challenges for their detection is the behaviour of the trigger algorithm for signals where very displaced vertices are involved. This has an impact on the experiment sensitivity to detect unknown LLPs. Furthermore, the high-luminosity LHC project aims to increase luminosity by a factor of 10 respect to initial LHC's design in order to observe rare new phenomena. In this scope, track reconstruction in real-time will be crucial for LHCb trigger systems when dealing with the large amount of hits in the different subdetectors. Dedicated track reconstruction algorithms have been developed in order to cope with the large data output from proton-proton collision. One example is the *HybridSeeding*, which has been successfully introduced in the LHCb trigger. Great effort is being made to speed up the performance of such algorithm by adopting a GPU-based solution for the first stage of the High Level Trigger. Other strategies take advantage of field-programmable gate array (FPGA) devices, which introduce parallel computational capabilities with a low energy consumption. In this work we evaluate the performance of the current LHCb trigger algorithm for LLP signals and propose new strategies to increase the experiment sensitivity for NP involving LLPs. Moreover, we inspect some features of the *HybridSeeding* algorithm by using FPGA architectures and introducing Artificial Intelligence strategies.

IFIC Contributions to the Computing of the ATLAS Experiment for the Run 3 of the LHC

Carlos García Montoro*, Javier Alberto Aparisi Pozo, Álvaro Fernández Casaní, Esteban Fullana Torregrosa, Santiago González de la Hoz, José Salt Cairols, Javier Sanchez, Miguel Villaplana Perez

Instituto de Física Corpuscular (IFIC), centro mixto CSIC – UV. Catedrático José Beltrán 2, 46980 Paterna, Spain.

*e-mail: carlos.garcia@ific.uv.es

Worldwide LHC Computing Grid (WLCG) sites around the world have been preparing for Run 3, updating their storage and computational resources, as well as their networking. After a budget reduction, the Spanish contribution to the ATLAS Tier2s was lowered from 4% to 3%. Spain has a federated Tier2 (IFIC, IFAE and UAM), where IFIC holds 60% of the resources [1]. IFIC's Tier2 facility is considered a *Nucleus* by the ATLAS Collaboration, i.e. a Tier2 with a large amount of storage and network connectivity that can pass job production on to smaller *Satellite* Tier2s. IFIC provides in-house resources, resources using HPC facilities for simulation, and R&D to the experiment through the ATLAS EventIndex project [3].

Year	2016	2017	2018	2019	2020	2021	2022
CPU (HS06)	14150	20304	27840	33408	31008	27907	45000
Disk (TB)	1800	1872	2112	2430	2592	2235	3480

Table 1. IFIC Pledge 2016 – 2022.

IFIC in-house resources have been increased to yearly satisfy the compromised pledge shown in Table 1. At the end of 2021 IFIC was providing 50,720 HS06 of which around 25% were being provided by servers older than 6 years that are being replaced. Regarding storage, IFIC was providing 3,402 TiB. 2 PiB of them in servers older than 6 years that are being replaced too. The bandwidth has been updated from 2x10 Gbps to a 100 Gbps connection to UV backbone. IFIC is ready for RedIRIS-Nova at 100 Gbps.

IFIC has also provided computing resources to the ATLAS Collaboration through HPC resources of the *Red Española de Supercomputación (RES)*. Between 2018 and 2020 IFIC applied for resources via RES standard calls. At that time IFIC obtained opportunistic resources from Lusitania. Since mid 2020 there has been an agreement with the BSC that grants resources from MareNostrum 4 to the LHC computation community [2]. Thanks to this agreement, around 10 million hours are granted every quarter at BSC for ATLAS. We are able to use these resources for simulation using singularity containers that are pre-placed at MareNostrum.

IFIC has been steadily providing more that 5,000 running job slots since 2019. They can be either single-core or multi-core with 8 cores and they typically use 2 GiB per job slot. Around 2,000 additional job slots are provided by MareNostrum 4 as shown in Figure 1. With all these resources, more than 300 billion events have been processed in the last 5 years.

IFIC also plays a key role in ATLAS EventIndex, the catalogue of all ATLAS events. IFIC coordinates the data production and is in charge of the data collection. EventIndex has evolved to cope with the data production rates expected for Run 3[3]. IFIC has designed and developed an architecture that replaces the original HDFS-based storage with a new one based on HBase and Phoenix. Figure 2 shows the cumulative amount of event records processed by EventIndex.

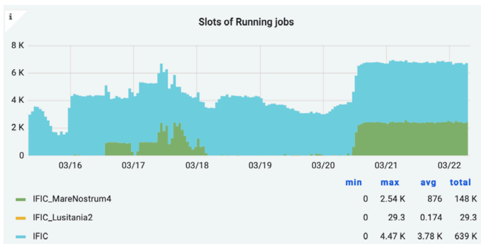

Figure 1. Slots of Running jobs (IFIC + HPC)

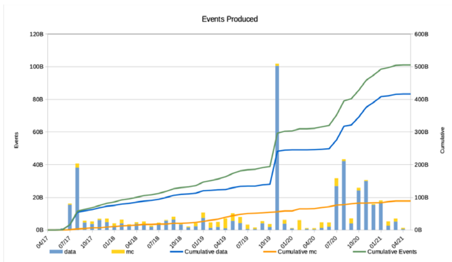

Figure 2. Event records processed by EventIndex.

[1] Santiago González de la Hoz et al., *EPJ Web Conf.* **245**, 07027 (2020).
[2] Carles Acosta-Silva et al., *EPJ Web Conf.* **251**, 02021 (2021).
[3] Dario Barberis et al., The ATLAS EventIndex for LHC Run 3, *EPJ Web Conf.* **245**, 04017 (2020).

Exact electromagnetic duality with nonminimal couplings

Pablo A. Cano[1], **Ángel Murcia**[2,*]

[1] *Instituut voor Theoretische Fysica, KU Leuven. Celestijnenlaan 200D, B-3001 Leuven, Belgium.*
[2] *Instituto de Física Teórica UAM/CSIC. C/ Nicolás Cabrera 13-15, C.U. Cantoblanco, E-28049 Madrid, Spain.*

*e-mail: angel.murcia@csic.es

We study nonminimal extensions of Einstein-Maxwell theory with exact electromagnetic duality invariance. Any such theory involves an infinite tower of higher-derivative terms whose computation and summation usually represents a challenging problem. Despite that, we manage to obtain a closed form of the action for all the theories with a quadratic dependence on the vector field strength. In these theories we find that the Maxwell field couples to gravity through a curvature-dependent susceptibility tensor that takes a peculiar form, reminiscent of that of Born-Infeld Lagrangians. We study the static and spherically symmetric black hole solutions of the simplest of these models, showing that the corresponding equations of motion are invariant under rotations of the electric and magnetic charges. We compute the perturbative corrections to the Reissner-Nordström solution in this theory, and in the case of extremal black holes we determine exactly the near-horizon geometry as well as the entropy. Remarkably, the entropy only possesses a constant correction despite the action containing an infinite number of terms. In addition, we find there is a lower bound for the charge and the mass of extremal black holes. When the sign of the coupling is such that the weak gravity conjecture is satisfied, the area and the entropy of extremal black holes vanish at the minimal charge.

quantumfdtd, a computational framework for the Relativistic Schrödinger Equation

Rafael Delgado Lopez[1,*], Sebastian Steinbeißer[2], Michael Strickland[3], Johannes Heinrich Weber[4]

[1] *Matemática Aplicada a las TIC, ETSIS de Telecomunicación (UPM), Campus Sur, 28031 Madrid, Spain.* [2] *Physik-Department, Technische Universität München (TUM), D-85748 Garching b. München, Germany.* [3] *Department of Physics, Kent State University, Kent, OH 44242, USA.* [4] *Institut für Physik & IRIS Adlershof, Humboldt-Universität zu Berlin, Zum Großen Windkanal 6, D-12489 Berlin, Germany*

*e-mail: rafael.delgado@upm.es

We present work [1], in which we extend the publicly available quantumfdtd code. It was originally intended for solving the time-independent three-dimensional Schrödinger equation via finite-difference time-domain (fdtd) method and extracting the ground, first and second excited states. We extend it to (a) include the case of the relativistic Schrödinger equation and (b) add two optimized FFT-based kinetic energy terms for the non-relativistic case. All the three new kinetic terms (the two non-relativistic and the relativistic one) are computed using Fast Fourier Transform (FFT). We release the resulting code as version 3 of quantumfdtd. Finally, the original code now supports arbitrary external file-based potentials and the option to project out distinct parity eigenstates from the solutions.

Most quark models used for phenomenological descriptions of QCD bound states are described by the three-dimensional Schrödinger equation with different potentials. In particular, these models have successfully describe below-threshold charmonium production and bottomonium spectra and have helped to establish confidence in QCD as the first-principles description of hadronic matter [2–4]. Non-relativistic effective field theory methods have been used for a first-principles approach to potential-based non-relativistic QCD (pNRQCD) [5,6]. In order to describe quarkonium evolution in the quark-gluon plasma, these potential models have been extended to finite temperature [7–9] and non-equilibrium [10–14]. In the last case, the potentials are no longer real-valued or spherically symmetric. In the full non-equilibrium case, a full three-dimensional solver, like the one developed in this work, is necessary.

[1] R.L.Delgado, S.Steinbeißer, M.Strickland, J.H.Weber, Comput.Phys.Commun.**272** (2022) 108250
[2] D.Ebert, R.N.Faustov, V.O.Galkin, Phys.Rev.D**67** (2003) 014027
[3] E.Eichten, S.Godfrey, H.Mahlke, J.L.Rosner, Rev.Mod.Phys.**80** (2008) 1161–1193
[4] J.Segovia, P.G.Ortega, D.R.Entem, F.Fernández, Phys.Rev.D**93** (7) (2016) 074027
[5] N.Brambilla, A.Pineda, J.Soto, A.Vairo, Nucl.Phys.B**566** (2000) 275; Phys.Rev. D**60** (1999) 091502
[7] M.Laine, O.Philipsen, P.Romatschke, M.Tassler, J.High Energy Phys.**03** (2007) 054
[8] N.Brambilla, J.Ghiglieri, A.Vairo, P.Petreczky, Phys.Rev.D**78** (2008) 014017; Phys.Rev.D**82** (2010) 074019
[10] A.Dumitru, Y.Guo, M.Strickland, Phys.Lett.B**662** (2008) 37–42
[11] Y.Burnier, M.Laine, M.Vepsalainen, Phys.Lett.B**678** (2009) 86–89
[12] A.Dumitru, Y.Guo, M.Strickland, Phys.Rev.D**79** (2009) 114003
[13] A.Dumitru, Y.Guo, A.Mocsy, M.Strickland, Phys.Rev.D**79** (2009) 054019
[14] Y.Guo, L.Dong, J.Pan, M.R.Moldes, Phys.Rev.D**100** (3) (2019) 036011

Acknowledgements: The code was extensively used and tested in the Computational Physics II online course at the Humboldt-Universität Berlin in winter semester 2020/21 (course by A.Patella and J.H.Weber). R.L.Delgado was supported by the Ramón Areces Foundation post-doctoral fellowship, the INFN post-doctoral fellowship AAOODGF-2019-0000329 and the Spanish grant MICINN: PID2019-108655GB-I00. M.Strickland was supported by the U.S. Department of Energy, Office of Science, Office of Nuclear Physics Award No. DE-SC0013470. J.H.Weber was supported by the U.S. Department of Energy, Office of Science, Office of Nuclear Physics and Office of Advanced Scientific Computing Research within the framework of Scientific Discovery through Advanced Computing (SciDAC) award Computing the Properties of Matter with Leadership Computing Resources. His research was funded by the Deutsche Forschungsgemeinschaft (DFG, German Research Foundation) - Projektnummer 417533893/GRK2575 "Rethinking Quantum Field Theory". We acknowledge the support by the Deutsche Forschungsgemeinschaft (DFG, German Research Foundation) under Germany's Excellence Strategy – EXC-2094 – 390783311 via the Excellence Cluster "ORIGINS". The simulations have been carried out on the computing facilities of the C2PAP and the Leibniz Supercomputing Center (SuperMUC), on the local theory cluster of the Physics Department of TUM, and on the local cluster at the INFN-Firenze.

Is gravitational collapse possible in $f(R)$ gravity?

Adrián Casado-Turrión[1,*], Álvaro de la Cruz-Dombriz[2,3], Antonio Dobado[1]

[1] *Departmento de Física Teórica and Instituto IPARCOS, Universidad Compltense, 28040 Madrid, Spain.* [2] *Departamento de Física Fundamental, Universidad de Salamanca, 37008 Salamanca, Spain.* [3] *Cosmology and Gravity Group, Department of Mathematics and Applied Mathematics, University of Cape Town, Rondebosch 7700, Cape Town, South Africa.*

*e-mail: adricasa@ucm.es

Gravitational collapse is still poorly understood in the context of $f(R)$ theories of gravity. The main reason for this is that junction conditions in these models are different and much more stringent than their counterparts in General Relativity. As a result, the most paradigmatic description of gravitational collapse in Einstein gravity, the Oppenheimer-Snyder model, is known not to be a solution of $f(R)$ theories of gravity, neither in their metric nor Palatini formulations. The smooth matching between the metrics inside and outside the stellar surface (which is possible in General Relativity) is no longer allowed by the junction conditions of $f(R)$ gravity.

For these reasons, we have endeavoured to shed some light on the issue of gravitational collapse in $f(R)$ gravity by means of a systematic treatment of the relevant junction conditions [1]. After thoroughly discussing how the Oppenheimer-Snyder construction should be generalised to fit within $f(R)$ gravity, we shall subsequently proceed to explore the existence of novel exterior solutions compatible with physically viable interiors. We will show that some paradigmatic vacuum metrics cannot represent spacetime outside a collapsing dust star in metric $f(R)$ gravity. In particular, we have found that, in $f(R)$ theories, the exterior solution must be strikingly different from the Schwarzschild metric, which is the only possible exterior spacetime in General Relativity, as per Birkhoff's theorem.

[1] Adrián Casado-Turrión, Álvaro de la Cruz-Dombriz, Antonio Dobado, accepted for publication in *Physical Review D* (2022), arXiv:2202.04439 [gr-qc].

Two lines of space reserved to include
codes of the symposium and of this communication

Search for flavourful 2HDM model in multilepton plus multi-b-jets final states

Merve Nazlim Agaras[1], Noemi Cavalli[3], **Shalini Epari**[1,*], Aurelio Juste Rozas[1], Stergios Kazakos[1], Javier Montejo Berlinger[2], Nicola Orlando[1], Tamara Vázquez Schroeder[2]

[1]*IFAE-Barcelona, Spain.*
[2]*CERN, Switzerland.*
[3]*University of Bologna, Italy - TU Dortmund, Germany.*

*e-mail: shalini.epari@cern.ch

A search for flavour violating heavy Higgs bosons decaying to multilepton plus multi-b-jets final states is performed using the full Run-2 dataset collected at $\sqrt{s}$ = 13 TeV with integrated luminosity of 139 fb^{-1}, by the ATLAS experiment at the LHC. The target model is an extension of the Standard Model (SM) with the addition of a second complex Higgs doublet (two-Higgs-doublet model, or 2HDM), giving rise to five Higgs bosons: two CP-even scalar fields (h and H), one CP-odd pseudo-scalar (A) and two charged Higgs ($H^{\pm}$) - without the requirement of a discrete Z_2 symmetry. In the alignment limit, the target model predicts flavour changing neutral currents in the heavy Higgs sector while respecting the SM-like nature of the $h(125)$ particle discovered at the LHC [1].

The analysis considers the production of the heavy scalar (pseudo-scalar) and has four degrees of freedom: the mass of the BSM Higgs $m_H(m_A)$ and ρ_{tq} (the coupling between the top and up/charm or another top quark). The various 2HDM signal types explored lead to final states with same-sign tt, ttq, $tttq$, three top and four top quarks (Figure 1). Benchmark couplings (ρ_{tt} = 0.27 and ρ_{tq}= 0.14) are chosen such that the model explains the excesses seen in previous ATLAS analyses, namely the $t\bar{t}H/t\bar{t}W$ analysis which fits the normalisation of the $t\bar{t}W$ background 60% above the next-to-leading order (NLO) prediction [2], and a dedicated search for that fits a normalisation a factor of two above the NLO prediction [3]. Further, 2HDM models with extra top Yukawa couplings are phenomenologically interesting since they can explain the generation of the baryon asymmetry of the universe [4].

Events are selected with at least two jets and at least one jet tagged as a b-jet. Events are then categorised depending on the multiplicity of light leptons (electron and muon) into channels (same-sign 2l, 3l and 4l channels). A deep neural network (DNN)-based categorisation is used to enhance the purity of each 2HDM signal. The Monte Carlo predictions of the dominant background are corrected and validated using dedicated control and validation regions. Finally, dedicated DNN are trained to discriminate signal from background in each of the signal categories and are used as final discriminants in the fit. A maximum-likelihood fit is performed on all the bins in the control and signal region event categories, to determine the 2HDM signal cross-section (considering all processes together: same-sign tt, ttq, $tttq$, three top and four top) and the normalisation factors for the major irreducible background processes and fake-lepton processes. In absence of an excess above the SM prediction, 95% confidence level limits are derived on model parameters for different benchmark scenarios. This is the first search at the LHC for such flavourful heavy Higgs bosons.

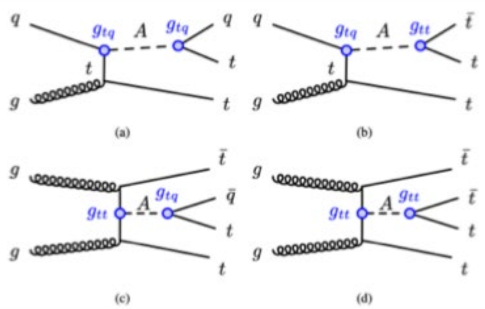

Figure 1. Representative Feynman diagrams for the dominant production and decay modes of the heavy (pseudo-)scalars considered in the analysis.

[1] W.-S, Hou and M. Kikuchi, Approximate Alignment in Two Higgs Doublet Model with Extra Yukawa Couplings, *EPL* **123**, 11001 (2018).

[2] ATLAS Collaboration, Analysis of $t\bar{t}$H and $t\bar{t}$W production in multi-lepton final states with the ATLAS detector, ATLAS-CONF-2019-045.

[3] ATLAS Collaboration, Evidence for $t\bar{t}t\bar{t}$ production in the multiple-ton final state in proton-proton collisions at $\sqrt{s}$=13 TeV the ATLAS detector, *Eur. Phys. J. C* **80**, 1085 (2020).

[4] K. Fuyuto, W.-S, Hou and E. Senaha, Electroweak baryogenesis driven by extra top Yukawa couplings, *Phys. Lett. B* **776**, 402 (2018).

Measurement of the quadruple-differential angular decay rates of single top quarks produced in the t-channel at $\sqrt{s}$=13 TeV

Mariam Chitishvili[1,*], Maria Jose Costa Mezquita [1], Carlos Escobar Ibañez[1]

[1] *Instituto de Fisica Corpuscular (IFIC), Centro Mixto Universidad de Valencia - CSIC, Valencia, Spain*
*e-mail: Mariam.Chitishvili@ific.uv.es

The fact that the top-quark lifetime $\mathcal{O}(10^{-25}\text{s})$ is smaller than its hadronisation time scale $\mathcal{O}(10^{-24}\text{s})$ allows this quark to be studied like a free quark. In addition, as its lifetime is also shorter than depolarisation time $\mathcal{O}(10^{-21}\text{s})$ and it decays almost exclusively via on-shell W boson and b quark ($t \to Wb$), the top-quark spin information is directly transferred to its decay products. Because of these exceptional properties, the top-quark production and decay kinematics represent an important probe of physics process beyond the Standard Model (SM).

The tWb vertex structure can be probed using single-top-quark t-channel events. This analysis uses an integrated luminosity of 139 fb^{-1} of proton-proton collision data at centre-of-mass energy of 13 TeV collected by the ATLAS detector during LHC Run 2. This analysis employs a novel model-independent framework proposed in [1] where the quadruple-differential top-quark decay rate, $\frac{1}{\Gamma}\frac{d\Gamma}{d\Omega d\Omega^*}$, is used to simultaneously determine the five generalised helicity fractions and two phases, the polarisation in three orthogonal directions of the produced top quark as well as the t-channel production cross-section.This differential decay (defined from transition amplitudes) can be expressed with orthonormal functions $M^{j_1 j_2}_{m'm}$ and angular coefficients $c^{j_1 j_2}_{m'm}$ that can be measured directly from data:

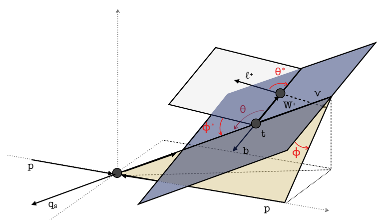

Figure 1. Definition of the four angles $(\phi, \theta, \phi^*, \theta^*)$ used in this analysis.

$$\frac{1}{\Gamma}\frac{d\Gamma}{d\Omega d\Omega^*} = \sum_{j_1 j_2 m' m} c^{j_1 j_2}_{m'm} M^{j_1 j_2}_{m'm}(\phi, \theta, \phi^*, \theta^*)^*,$$

where θ and ϕ are the spherical coordinates of the W boson momentum in the top-quark rest frame, θ^* and ϕ^* are the spherical coordinates of the charged-lepton momentum in the W-boson rest frame, and $d\Omega = \sin\theta d\theta d\phi$ and $d\Omega^* = \sin\theta^* d\theta^* d\phi^*$ are the solid angles in the top-quark and W-boson rest frame, respectively.

After measuring the physical quantities previously mentioned, it will be possible to set (the most) stringent limits to the relevant dimension-six Effective Field Theory (EFT) complex operators (C_{tW}, etc) of the tWb vertex [2]. On Fig. 2 one can see the expected sensitivity of the angular coefficients $c^{j_1 j_2}_{m'm}$ for various SM and non-SM predictions given by different generators.

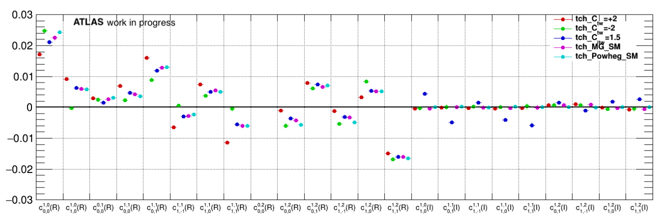

Figure 2. Angular coefficients measured from two SM and three different EFT-varied predictions, provided by different generators, demonstrating which coefficients could be sensitive to the new physics.

Deviations from SM-expected values would provide hints of physics beyond the SM, and furthermore, complex values could imply that the top-quark decay has a CP-violating component.

[1] J. A. Aguilar-Saavedra, J. Boudreau, C. Escobar, and J. Mueller, *Eur. Phys. J. C* **77**, (2017).
[2] M. de Beurs, E. Laenen, M. Vreeswijk, E. Vryonidou, *Eur. Phys. J. C* **78**, (2018).

Two lines of space reserved to include
codes of the symposium and of this communication

Search for associated production of a Higgs boson and a single-top quark in the $2\ell+\tau_{had}$ final state at 13 TeV in ATLAS

S. Cabrera [1], C. Escobar[1], J. Guerrero[1], **P. Martínez-Agulló**[1,*]

[1] *Instituto de Física Corpuscular (IFIC), Centro Mixto Universidad de Valencia - CSIC, Valencia, Spain*

*e-mail: pablo.martinez.agullo@ific.uv.es

The discovery of a Higgs boson by the ATLAS and CMS experiments in 2012 opened a new field for exploration in the realm of particle physics. In order to better understand the Standard Model (SM) of particle physics, it is of prominent interest to understand the Yukawa coupling of the Higgs boson to the top quark (y_t), being the latter the most massive fundamental particle and, consequently, the one with the largest coupling to the Higgs boson.

The direct measurement of y_t is only possible at the LHC via two associated Higgs productions: with a top-quark-antiquark pair ($t\bar{t}H$) and with a single-top quark (tH). While the $t\bar{t}H$ just permits the determination of the magnitude of y_t, the only way of directly measuring its sign is through the tH production (Fig. 1). This is due to the fact that the two leading order Feynman diagrams for the tH production interfere with each other depending on the y_t sign. Current experimental constrains on y_t favour the SM predictions, but an opposite sign with respect to the expectations of the SM is not completely excluded yet [2].

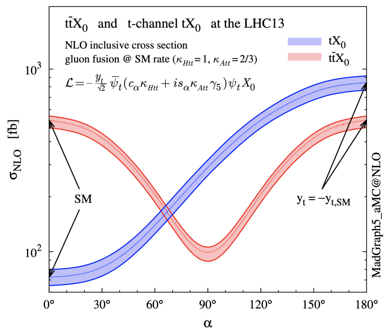

Figure 1. Production cross-section as a function of the CP mixing angle, α, at NLO for tX_0 and $t\bar{t}X_0$, where X_0 represents a Higgs boson [1].

In this work it is presented a search for the tH production in a final state with two light-flavoured-charged leptons (electrons or muons) and one hadronically-decaying tau lepton (named $2\ell+\tau_{had}$ channel). This analysis uses an integrated luminosity of 139 fb^{-1} of proton-proton collision data at centre-of-mass energy of 13 TeV collected by the ATLAS detector during LHC Run 2.

This search is exceptionally challenging due to the extremely small cross-section of the tH process (70 fb), and of the $2\ell+\tau_{had}$ final-state channel, in particular, which only accounts for a 3.5% of the total tH production. Therefore, the separation of the tH signal events from background events is done by means of machine-learning (ML) techniques using boosted-decision trees (BDT) to define both signal (Fig. 2) and control regions to constrain the most important background processes, which are those related to top-quark-antiquark-pair production without and with and additional boson ($t\bar{t}$, $t\bar{t}H$, $t\bar{t}W$ and $t\bar{t}Z$) and Z boson plus jets.

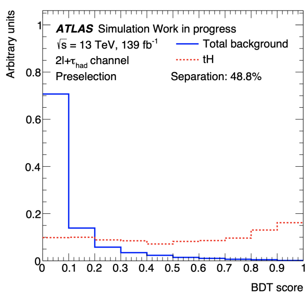

Figure 2. Score of the BDT targeting tH events over all backgrounds, used to define the signal region.

Significant suppression of the background events with jets wrongly selected as leptons or non-prompt leptons originating from heavy-flavour decays is achieved by demanding electrons and muons to pass strict identification and isolation requirements. Simultaneously, hadronic-τ leptons are demanded to pass the requirement of a recurrent-neural-network-based discriminator to reduce misidentifications from jets.

The reconstruction of the events is also enhanced by similar ML methods since in the scenario in which the light-flavour leptons have the same sign, a priori, it is not possible to determine which lepton is originated from the Higgs boson and which from the top quark.

The possible observation of an excess of signal events with respect to the SM prediction, would be an evidence of new physics in terms of CP-violating y_t coupling.

[1] F. Demartin, F. Maltoni, K. Mawatari and M. Zaro, *Eur. Phys. J. C* **75** (2015) 267.
[2] CMS Collaboration, *Eur. Phys. J. C* **81** (2021) 378

Search for associated production of a Higgs boson and a single top quark in 3l and 2lSS final states at 13 TeV in ATLAS

Susana Cabrera Urban, Carlos Escobar, **Jesús Guerrero Rojas***, Pablo Martínez-Agulló

[1]*Instituto de Física Corpuscular (IFIC), Centro mixto Universitat de València – CSIC, Valencia, Spain.*

*e-mail: jguerrero@ific.uv.es

The status of the search to produce a Higgs boson in association with a single top quark (*tH*) in multi-lepton final states is presented. The study uses an integrated luminosity of 139 fb^{-1} of LHC collision data at centre-of-mass-energy of 13 TeV, recorded by the ATLAS experiment. Three final states, targeting Standard Model (SM) Higgs bosons decaying to *WW**, *ZZ** and $\tau\tau$, are examined.

As for today, this is the only analysis sensitive to both the magnitude and the sign of the Yukawa coupling (y_t) of the Higgs boson to the top quark and the first direct search of *tH* production in the ATLAS collaboration. The *tH* process has an extremely low production cross-section (70 fb at $\sqrt{s} =$ 13 TeV), which originates from the destructive interaction of the diagrams where the Higgs couples to the top quark with those where the Higgs couples to the W boson. Other SM processes giving rise to similar final states and conforming the main background of this search, have production cross-sections up to seven times higher than that of *tH*. This is the case for the associated production of a Higgs boson and a pair of top quarks (*ttH*). This fact makes multivariate analysis methods a key tool to distinguish signal events from the diverse large backgrounds. This search is also sensitive to CP-violation since, as shown in Figure 1 (blue line), the cross-section could be up to 10 times higher in the completely inverted hypothesis with respect to the SM prediction (CP mixing angle, α, equal to 180^0) [1]. All these features make this search very challenging and this process exceptionally sensitive to deviations from SM predictions.

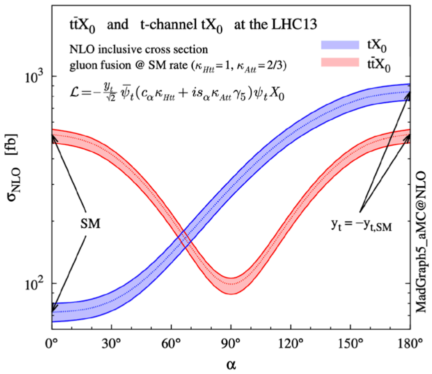

Figure 1. Production cross-section as a function of CP mixing angle α , at NLO for tX_0 and ttX_0 where X_0 represents a Higgs boson [1].

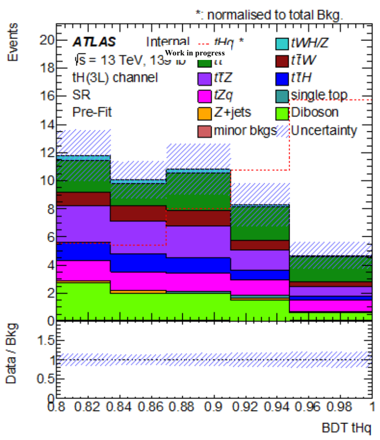

Figure 2. Signal region enriched in *tH*. This region is completely blinded to data.

Two final states are studied in this work: three leptons (3l) and two leptons same-sign (2lSS) where only electrons and muons are considered. The hadronically decaying taus are explicitly vetoed. Several enriched regions for the signal and the main backgrounds, as the *tH*-enriched signal region in Figure 2, are defined to estimate the signal strength ($\mu(tH)$) in both channels. The signal strength is defined as the ratio of the measured number of events of a given event sample and the number of events predicted by the SM. Currently, the expected $\mu(tH)$ for each channel are: $\mu(tH) < 8.1$ for the 2lSS final state, and $\mu(tH) < 14.1$ for the 3l final state both at 95% confident level, including all systematics and statistical uncertainties.

[1] F. Demartin, F. Maltoni, K. Mawatari, and M. Zaro. *Eur. Phys. J. C* **75**, 267 (2015).

Two lines of space reserved to include
codes of the symposium and of this communication

Search for long-lived neutral particles in pp collisions at $\sqrt{s} = 13$ TeV that decay into displaced hadronic jets in the ATLAS calorimeter

Emma Torró Pastor[1], **Mariia Didenko**[1,*], Victoria Sánchez Sebastián[1]

[1] *Instituto de Física Corpuscular (IFIC), Centro Mixto Universidad de Valencia - CSIC, Valencia, Spain.*

*e-mail: mariya.didenko@cern.ch

Many Beyond the Standard Model (SM) theories predict the existence of new particles whose lifetimes can be long enough for them to travel a macroscopic distance before decaying. Long-lived particles (LLPs) are allowed in theories such as supersymmetric or neutral naturalness models which feature Hidden Sector (HS) [1] that address the hierarchy problem. The sensitivity of a given search to detect LLPs depends on its nature (neutral or charged) and the decay length (promptly decaying or displaced). The decay of a LLP created in proton-proton collisions in the ATLAS experiment could produce various highly unconventional signatures in the detector.

The analysis presents a search for neutral LLPs decaying hadronically in the ATLAS calorimeters [2]. A benchmark HS model is studied, where neutral long-lived scalar particles with masses ranging from 5 GeV to 475 GeV are produced in pairs from the decay of the mediator with masses between 60 GeV and 1000 GeV. If the scalar decay occurs in the calorimeters, the two resulting quarks are reconstructed as a single jet with unusual features compared to SM jets (see Fig. 1).

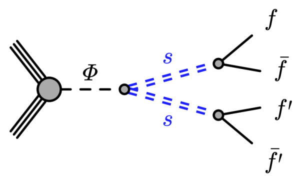

Figure 1: A diagram showing the $\Phi \to ss \to f\bar{f}f'\bar{f}'$ decay used as the benchmark model.

These jets will often have a high ratio of energy deposited in the Hadron Calorimeter (E_H) to energy deposited in the Electromagnetic Calorimeter (E_{EM}), $E_H\ /E_{EM}$ referred to as the CalRatio. CalRatio jet candidates are first selected by dedicated LLP signature-driven triggers specifically designed for this search. Then, different machine learning techniques such as a neural network (NN) are used to identify displaced jets. In particular, a deep NN is used to predict whether candidate jets are produced by a LLP decay or from the expected sources of background: SM multijets, beam-induced background (BIB) and cosmic rays, and an adversarial training is applied to minimize the impact of Monte Carlo (MC) mismodeling. The use of this NN implies a noticeable improvement in sensitivity compared to the previous version of this search [3]. This is specially the case for low-mass mediators giving rise to low-p_T LLPs, with a challenging discrimination from BIB. MC simulations are not robust in predicting such unconventional signatures. Therefore, the analysis uses data-driven techniques for the background estimation.

The analysis uses the full LHC Run 2 dataset of 13 TeV collisions, corresponding to an integrated luminosity of 139 fb^{-1}. No significant excess of events in the signal region is observed with respect to the data-driven background prediction. The improvements to the analysis and additional data led to an extension of the limits for mediator masses above and below 200 GeV by a factor of around 1.5-2 and 3-5, respectively, compared to the previous version of the analysis [3].

For models with a SM-like Higgs boson mediator, branching fractions to neutral scalars above 10 % are excluded between approximately 2 cm and 12 m in the LLP mean proper lifetime ($c\tau$), depending on the scalar's mass (see Fig. 2).

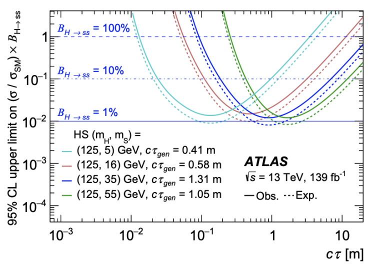

Figure 2: Summary of 95 % CL expected and observed limits on the branching fraction of a Higgs-like mediator to pairs of neutral LLPs considered in this analysis [2]

[1] M. J. Strassler and K. M. Zurek, *Phys. Lett. B* **651**, (2007).

[2] ATLAS Collaboration, arXiv:2203.01009 [hep-ex], Submitted to JHEP (2022).

[3] ATLAS Collaboration, *Phys. Rev. D* **99**, 052005 (2019).

Two lines of space reserved to include
codes of the symposium and of this communication

Electromagnetic tensor endowed with polarimetric parameters: application to the vicinity of extremely dense bodies

J. C. Martin[1], **L. Remón**[1,*], M. Pawlowska[2]

[1]*Departamento de Física Aplicada, Universidad de Zaragoza, C/ Pedro Cerbuna, 12 50009, Zaragoza, España.*
[2]*Department of Theoretical Physics, Wroclaw University of Science and Technology 27 Wybrzeże Wyspiańskiego st., 50-370 Wrocław, Poland.*

*e-mail: lauremar@unizar.es

Electromagnetic flux analysis in the vicinity of mass density singularities constitutes a challenging question. A relativistic treatment based on an adaptation of the Einstein universe equations to an anisotropic Minkowski space has been implemented. The procedure proposed allows one not only to predict the so-called relativistic lens effects, with good agreement with previous formalisms [1] but also to include polarimetric information in the electromagnetic tensor. It is shown that the system quadri-eigenfunction can be approximately assessed by formal analogy to the Navier-Stokes (NS) equations in the case of spherical symmetry. Numerical solutions have also been obtained for different mass density elliptical distributions. In particular, the polarimetric space-time evolution has been analysed, for the first time to our knowledge.

A three-dimensional projection of the solutions can be generated by means of the ray tracing and commercial optical software (ZEMAX, OpticStudio 21.2.1). In order to do so, the complex 3 x 3 $n(\xi)$ refractive index tensor representing the medium properties (ξ being the non-angular oblate spherical coordinate) has been locally adapted by means of an equivalent real, scalar refractive index distribution combined with Jones matrixes formalism, thanks to a procedure specifically developed for this work. Figure 1 shows several trajectories obtained for spherical symmetry, in order to show the agreement between the general method and the NS approximation. Figure 2 shows polarization evolution corresponding to Figure 1 trajectories, where chirality can be appreciated.

The strong influence of the mass gradients in the electromagnetic wave polarimetric behaviour may be a powerful tool for the study of extremely dense matter distributions.

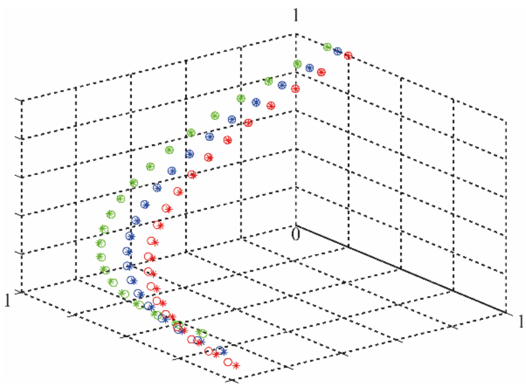

Figure 1. Ray tracing in a medium with mass density distribution $m(r)=\exp(-r^2)$, for three different initial conditions (red, blue and green). Dots: rigorous calculation. Circles: NS approximation.

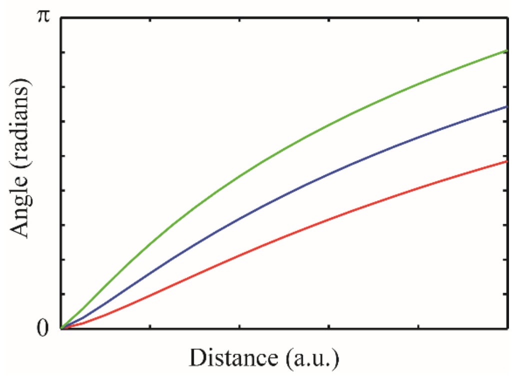

Figure 2. Rotation angle with regard to the initial polarization plane (color correspondence with Fig. 1). Positive angle means dextrogyre rotation.

[1] Sudarshan ECG, Simon R and Mukunda N, *Physical Review A* **28**, 2933 (1983).

Two lines of space reserved to include
codes of the symposium and of this communication

Prediction of symmetric partners of the $Z_c(3900)$ and $Z_b(10610)$ exotic states using heavy quark spin symmetry and $SU(3)$ flavor symmetry

Víctor Montesinos[1,*], Miguel Albaladejo[1], Juan Nieves[1]

[1] *Instituto de Física Corpuscular (centro mixto CSIC-UV), Institutos de Investigación de Paterna, C/Catedrático José Beltrán, E-46980 Paterna, Valencia, Spain*

*e-mail: vicmonte@ific.uv.es

In the last two decades some states have been found which present difficulties when trying to accommodate them to the conventional quark models, that is, to a three-quark structure in the case of baryons or to a quark-antiquark pair for mesons. Some recent examples in the meson spectrum are:

- **The isovector** $J^{PC} = 1^{+-}$ $Z_c(3900)$ **state.** It has a charm-anticharm component given that it is observed in the $J/\Psi\ \pi$ and $\bar{D}\ D^*$ spectra, but it is also found to be **charged** (it has isospin equal to one). This state was first seen by the BESIII collaboration in 2013, see Ref. [1].
- **The isovector** $J^{PC} = 1^{+-}$ $Z_c(4020)$ **state.** Similarly to the $Z_c(3900)$ it has a charm-anticharm component and is charged. First reported by the BESIII collaboration a short time after the $Z_c(3900)$, see Ref. [2].
- **The isovector** $J^{PC} = 1^{+-}$ $Z_b(10610)$ **and** $Z_b(10650)$ **states.** They have a bottom-antibottom component and are also charged. First seen by the BELLE collaboration, Ref. [3].
- **The isospin** $1/2$ $J^P = 1^+$ $Z_{cs}(3985)$ **state**. Reported by the BESIII collaboration in 2021 in the $\bar{D}_s D^*$ invariant mass, Ref. [4]. This state has a charm-anticharm component while simultaneously having strangeness.

All the states listed above need to be described by a minimum of four quarks (two quarks and two antiquarks), and are thus known as tetraquarks.

There exist several proposals for the "arrangement" of these four quarks, but among them the meson-antimeson molecule model is prominent given that the masses of these states lie very close to the $\bar{D}^{(*)}D^{(*)}$, $\bar{D}^{(*)}D_s^{(*)}$, $\bar{B}^{(*)}B^{(*)}$ or $\bar{B}_s^{(*)}B^{(*)}$ production energy thresholds. Using a meson-molecular model, we have performed a combined analysis of the $Z_c(3900)$, the $Z_c(4020)$, the $Z_{cs}(3985)$, the $Z_b(10610)$ and the $Z_b(10650)$ states. This combined analysis is made simple due to the existence of some symmetries: *Heavy Quark Spin-Flavor Symmetry* and the more usual $SU(3)$ *light quark flavor symmetry*. With this approach we are able to extend the results in Refs. [5,6] and predict the mass and width of three experimentally unseen states: one Z_{cs} and two Z_{bs} states. The masses of these states lie near the $\bar{D}^*D_s^*$, $\bar{B}_sB^* \simeq \bar{B}_s^*B$ and $\bar{B}_s^*B^*$ energy thresholds, respectively, and we expect these states to couple strongly to these channels.

[1] BESIII collaboration, *Phys. Rev. Lett.* **110**, 252001 (2013).
[2] BESIII collaboration, *Phys. Rev. Lett.* **111**, 242001 (2013).
[3] BELLE collaboration, *Phys. Rev. Lett.* **108**, 122001 (2012).
[4] BESIII collaboration, *Phys. Rev. Lett.* **126**, 102001 (2021).
[5] M. Albaladejo, F.-K. Guo, C. Hidalgo-Duque and J. Nieves, *Phys. Lett. B* **755**, 337 (2016).
[6] Z. Yang, X. Cao, F.-K. Guo, J. Nieves and M.P. Valderrama, *Phys. Rev. D* **103**, 074029 (2021).

Radiation hardness and timing performance of MALTA monolithic Pixel sensors in Tower 180 nm

Carlos Solans Sánchez

EP Department, CERN, Switzerland.

e-mail: carlos.solans@cern.ch

The MALTA family of depleted monolithic Pixel sensors have been produced in Tower 180 nm CMOS technology with small collection electrode and a novel asynchronous read-out that reduces the front-end power needs that allows to capture 100 MHit/s [1-3]. The challenge is to make this designs radiation hard to the levels of the inner trackers of the experiments at HL-LHC and beyond [4]. Prototypes have been produced with several process modifications to improve the charge collection. Starting from an n- blanket extends the junction to the full pixel size (standard), another one with a gap in the n- blanket (NGAP), and a third one with an extra deep p-well structure at the pixel edges (EDPW) [5]. Prototypes have been produced on high resistivity epitaxial silicon and on Czochralski substrates [6]. MALTA2 (Fig 1.) is the latest demonstrator of this family, and introduces a transistor in series (cascoded) to reduce the RTS noise and increase the gain of the front-end which is relevant for the uniform response of the matrix that does not contain an in-pixel threshold tuning mechanism. This technology is being developed at CERN in the context of the EP R&D and the AIDA innova programmes.

MALTA2 was extensively tested in particle beam tests at SPS CERN in 2021. Results will show its radiation hardness against 150 MRad TID and $2{\times}10^{15}$ 1 MeV n_{eq}/cm^2 NIEL. It will be presented how Czochralski substrates are better than epitaxial substrates for particle tracking at high doses due to the large charge collection that can be quantified by the size of the cluster. Additionally the Timing performance of the pixel will be evaluated with particle beams, where results will be shown on the average time of arrival of a hit to the collection electrode of the pixel. These are in line with the requirements of the bunch-crossing identification of the HL-LHC (25 ns), and not far away from those of the 15 ns bunch structure.

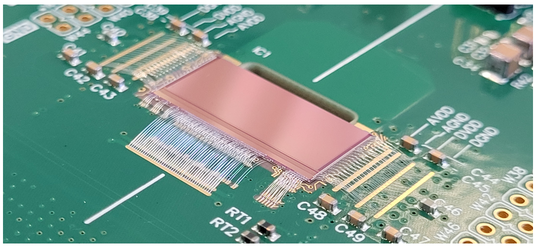

Figure 1. MALTA2 Monolithic Pixel detector.

[1] H. Pernegger et al, NIM A **986**, 164381 (2021) .
[2] M. Dyndal et al, JINST **15**, P02005 (2020).
[3] W. Snoeys et al, NIM A **871**, 90 (2017).
[4] E.J. Schioppa et al, NIM A **958**, 162404 (2020).
[5] M. Munker et al, JINST **14**, C05013 (2019).
[6] C. Solans et al, PoS ICHEP2020, 871 (2021).

Acknowledgements: This project has received funding from the European Union's Horizon 2020 Research and Innovation programme under GA no 101004761.

Technological Applications of Extensive Air Showers Simulations

M. Suárez-Durán[1], C. Sarmiento-Cano[2], A.J. Rubio-Montero[3], A. Taboada[2], R. Pagán-Muñoz[3], R. Calderón-Ardila[2], L.A. Núñez[4], I. Sidelnik[5], **R. Mayo-García**[3,*], H. Asorey[2,6]

[1]*Université Libre de Bruxelles, Av. Franklin Roosevelt 50, 1050 Brussels, Belgium.* [2]*Instituto de Tecnologías en Detección y Astropartículas (ITeDA). Centro Atómico Constituyentes (CNEA/CONICET/UNSAM) Av. Gral. Paz 1499, 1450 Villa Maipú, Argentina.* [3]*Centro de Investigaciones Energéticas, Medioambientales y Tecnológicas (CIEMAT), Av. Complutense 40, 28040 Spain.* [4]*Universidad Industrial de Santander, Carrera 27 y Calle 9, 28231 Bucaramanga, Colombia.* [5]*Departamento de Física de Neutrones, Centro Atómico Bariloche (CNEA/CONICET) Av. Bustillo 9500, 8400 San Carlos de Bariloche, Argentina.* [6]*Departamento Física Médica, Centro Atómico Bariloche (CNEA) Av. Bustillo 9500, 8400 San Carlos de Bariloche, Argentina.*

*e-mail: rafael.mayo@ciemat.es

Atmospheric radiation is mainly produced during the interaction of high energy cosmic rays with the atmosphere. After the first interaction of these primary cosmic rays, a series of radiative and decay processes generate a collective process known as Extensive Air Shower (EAS), with up to 10 secondary particles per primary per GeV at the altitude of the maximum development, and continue evolving up to reach the ground level.

Bearing this in mind, to calculate the atmospheric radiation background is a very complex and demanding task. This computation is originated from the integration of all the secondary particles produced by the complete and modulated flux of cosmic rays that impinge on the atmosphere. For doing this we developed ARTI [1], a computational framework that takes advantage of the state-of-the-art radiation propagation and interaction codes, such as CORSIKA [2] and Geant4 [3], to trustworthily estimate the expected flux of radiation at any place in the World under real-time evolving atmospheric and geomagnetic conditions [4]. We are also capable to include the impacts produced during the sudden occurrence of transient astrophysical phenomena. As these calculations require a vast amount of computational resources, several approaches were adopted, such as the recent development of OneDataSim [5], a virtualized application to run ARTI at high-performance computing and cloud-based environments.

In this work, we show some of the implications and technological applications of our research, including results related to the precise calculation of the expected muon flux at underground laboratories, the mining prospecting and volcanoes risk assessment in muography, some new applications for precision agriculture and personal safe ward, and even how we are able to predict the occurrence of silent and non-silent errors at the new exascale supercomputers centres.

In addition, some results will be shown for the future ANDES underground laboratory. Thus, regarding the study of high energetic secondary particles at the tens of TeV scale for this lab background calculations and expected flux of muons for muography geophysical applications, the expected flux over an integration time of 1 year at different altitudes of the ANDES mountain profile will be presented.

In all those cases, the accuracy and statistical significance of previous results have been extended by using these new resources.

[1] C. Sarmiento-Cano *et al.*, arXiv:2010.14591 [astro-ph.IM] (2021).
[2] D. Heck *et al.*, Forschungszentrum Karlsruhe Report FZKA 6019 (1998).
[3] S. Agostinelli *et al.*, *Nucl. Instrum. Meth. A* **506**, 250 (2003).
[4] H. Asorey, L.A. Nuñez, M. Suárez-Durán, *Space Weather* **16**, 461 (2018).
[5] A.J. Rubio-Montero *et al.*, In 2021 Winter Simulation Conference Conf. Proc, 1-12 (2021).

Acknowledgements: This work has been partially funded by the Spanish Ministry of Science, Innovation, and Universities CODEC-OSE project (RTI2018-096006-B-I00) and the Comunidad de Madrid CABAHLA project (S2018/TCS-4423), both with European Regional Development Fund (ERDF). It also profited from funding received by the H2020 co-funded project European Open Science Cloud - Expanding Capacities by building Capabilities (EOSC-SYNERGY, No. 857647). Simulations carried out made also use of the computing facilities provided by CETA-CIEMAT and CIEMAT.

Commissioning and Monitoring of the Calorimeter sub-detector of LHCb experiment

Paula Garcia Moreno[1,2]

[1] *Departament de Física Quántica i Astrofísica, Institut de Ciències del Cosmos, Spain.* [2] *Universitat de Barcelona, Spain.*

*e-mail: paula.garcia.moreno@cern.ch

In the upcoming months the LHC will start running again after a three-year shutdown, with the aim of starting a new period of data taking with five times more luminosity (Run 3). Due to that fact, all the LHCb sub-detectors will need to adapt to the new conditions to operate successfully.

The Calorimeter sub-detector is in charge of measuring the energy and position of the electrons, photons and hadrons by reading their energy in the Calorimeter cells [1]. In this talk I will report about the work that has already been performed, the work that is under development and the future steps that are going to be done regarding the Calorimeter sub-detector commissioning and monitoring tasks. Specifically, I will explain in an intuitive way how the Calorimeter software was configured in order to show useful histograms obtained with the firsts runs of the new beams, the problems we faced while working and the solutions we finally encountered.

Finally, I will give a brief report about my work on deciding which mask shape (3x3 cells, 2x2 cells or Swiss Cross cells) is used to perform electromagnetic clusters in the Electromagnetic Calorimeter in the new upgrade conditions [2]. That decision is made taking into account which mask shape is giving a higher resolution in energy and in position.

[1] LHCb collaboration, *Photon and neutral pion reconstruction* **LHCb-2003-091**.

[2] Alexis Vallier, *Photon reconstruction optimisation for the LHCb detector upgrade*.

Acknowledgements: I would want to acknowledge LHCb collaboration and my research group in Institut de Ciències del Cosmos for all the support I received during my work.

Two lines of space reserved to include
codes of the symposium and of this communication

Simulation and reconstruction of scintillation light with X-ARAPUCA photodetectors in SBND

Rodrigo Alvarez Garrote*

Departamento de Investigación Básica, CIEMAT, Spain

e-mail: rodrigo.alvarez@ciemat.es

SBND is a time-projection chamber that collects ionisation electrons and scintillation photons from liquid argon (LArTPC). It will be located 110 m downstream the Booster Neutrino Beam target at Fermilab and it is currently under construction. The SBND physics program is focused on beyond the Standard Model searches (sterile neutrinos, heavy neutral leptons, light dark matter...) and neutrino-argon cross-sections.

The photodetection system (PDS) provides trigger capabilities, cosmic-rays rejection (a large background due to the near-surface detector location), and complementary calorimetry. The PDS includes PMTs and X-ARAPUCAsensors, a novel technology that features single photo-electron resolution at cryogenic temperatures with large area coverage in a cost-effective fashion.

Proper simulation of the light readout and reconstruction is key for a precise determination of the interaction time (t0) and energy reconstruction, thus improving background rejection. In this talk, we present the latest X-ARAPUCA energy and time resolution estimates using a full SBND detector simulation. These results are of great interest because future LArTPC experiments such as DUNE will use X-ARAPUCAs as their PDS.

Unitarized one-loop graviton-graviton scattering

Rafael Delgado Lopez[1,*], Antonio Dobado[2], Domènec Espriu[3]

[1] *Matemática Aplicada a las TIC, ETSIS de Telecomunicación (UPM), Campus Sur, 28031 Madrid, Spain.* [2] *Departamento de Física Teórica and Instituto IPARCOS Universidad Complutense de Madrid, 28040 Madrid, Spain.* [3] *Departament de Física Quàntica i Astrofísica and Institut de Ciències del Cosmos (ICCUB) Universitat de Barcelona, 08028 Barcelona, Catalonia, Spain*

*e-mail: rafael.delgado@upm.es

We analyze [1] the next to leading order (NLO) graviton-graviton scattering amplitude via the Inverse Amplitude Method (IAM), well known to low-energy QCD practitioners [2]. Like the electroweak chiral lagrangian, successfully used for low-energy QCD, the Einstein-Hilbert (EH) lagrangian is a non-linear and non-renormalizable theory whose most relevant operator is a dimension two one containing two derivatives of the dynamical lagrangian. Both lagrangians contain a dimensionful constant in four dimensions: f_π for the pion lagrangian and the Planck mass M_P for the EH lagrangian. However, the EH lagrangian describing gravity is a gauge theory.

We use the tree-level graviton-graviton scattering amplitude given in [3] and the NLO computation done by Dunbar and Norridge [4] using string theory methods. Only counterterms proportional to $\mathcal{R}^2$, $\mathcal{R}_{\mu\nu}\mathcal{R}^{\mu\nu}$ and $\mathcal{R}^{\gamma\delta}_{\alpha\beta}\mathcal{R}^{\alpha\beta}_{\gamma\delta}$ are needed [3]. On-shell (lowest order equations of motion) these counterterms vanish, so that the theory is UV finita at NLO.

Dispersion relation via the inverse amplitude method [2,5] are used to seek for hypothetical graviton-induced resonances similar to those appearing in QCD. We focus on the $++++$ and $----$ helicity channels and analyze the $J = 0$, 2 and 4 partial waves. We look for resonances on the second Riemann sheet as well as for artifacts in the first Riemann sheet. The study of these artifacts is necessary since their appearance can mean that the inverse amplitude method is being applied beyond its validity conditions.

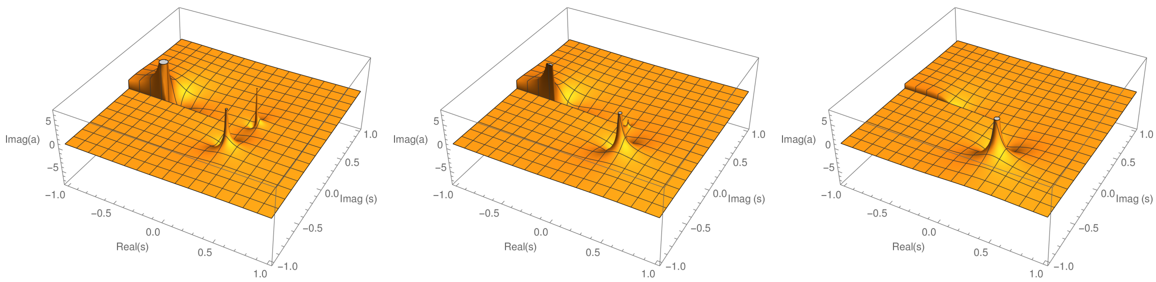

Figure 1: Figure from [1]. From top left, to right: plots of Imag a_0^{IAM} for different values of $\mu/M_p =$ 0.40, 0.35, 0.30. μ plays the role of an infrared cutoff [1]. See the dissapearance of the poles on the first Riemann sheet (quadrants I and II).

[1] R.L.Delgado, A.Dobado, D.Espriu, to appear on arXiv
[2] A.Dobado, J.R.Pelaez, Phys.Rev.D**56** (1997) 3057-3073
[3] G.'t Hooft, M.Veltman, Ann.Inst.H.Poincaré A**20** (1974), 69
[4] D.C.Dunbar, P.S.Norridge, Nucl.Phys.B**433** (1995), 181-208
[5] Rafael L.Delgado, A.Dobado, F.J.Llanes-Estrada, Phys.Rev.D**91** (2015) 7, 075017

Acknowledgements: R.L.Delgado was supported by the Ramón Areces Foundation post-doctoral fellowship, the INFN post-doctoral fellowship AAOODGF-2019-0000329 and the Spanish grant MICINN: PID2019-108655GB-I00.

Two lines of space reserved to include
codes of the symposium and of this communication

Gravitational particle production in the laboratory

Álvaro Parra-López[1,*], Jose A. R. Cembranos[1], Stefan Floerchinger[2], Tobias Haas[2], Natalia Sánchez-Kuntz[2], Mireia Tolosa-Simeón[2]

[1] *Departamento de Física Teórica and IPARCOS, Facultad de Ciencias Físicas, Universidad Complutense de Madrid, Ciudad Universitaria, 28040 Madrid, Spain.*
[2] *Institut für Theoretische Physik, Universität Heidelberg, Philosophenweg 16, 69120 Heidelberg, Germany.*

*e-mail: alvaparr@ucm.es

Considering quantum field theory in a general spacetime results in the appearance of phenomena such as the Unruh effect or Hawking radiation. In particular, the temporal variation of the geometry leads to the production of particles. This mechanism will be present as long as there exist a matter field that feels the time evolution of spacetime, and can explain, for example, the observed abundance of dark matter particles as a result of the heavy expansion carried out during inflation [1]. Since direct detection of such process seems unreachable, the use of *simulators* of these cosmological scenarios has been proposed. This is the main objective of the **analog gravity** field: To reproduce the dynamics of the field in certain geometry using as model a system that can be realized in the laboratory. The most extended analogy makes use of a weakly interacting Bose-Einstein condensate, described by the complex field Φ,

$$\Phi = \text{background} + \text{fluctuations} = \sqrt{n_0}e^{iS_0} + \frac{1}{\sqrt{2}}\left(\phi_1 + i\phi\right). \tag{1}$$

The system can be adjusted such that the imaginary part of the phononic fluctuations ϕ on top of its ground state behave as a massless scalar field in a flat FLRW universe.

Our work generalizes this analogy to FLRW universes with non-zero spatial curvature κ [2]. At the same time, we provide suitable observables in terms of the density contrast that can be used to detect particle production in a real experiment, as seen in [3]. The connection between the known theoretical result for the spectrum of produced particles S_k [4] and the laboratory comes from the proportionality $\delta_c \sim \dot{\phi}$, where $\delta_c(t, \boldsymbol{r}) \propto \sqrt{n_0(r)}\,[n(t, \boldsymbol{r}) - n_0(r)]$ is the density contrast and $n(t, \boldsymbol{r}) = |\Phi(t, \boldsymbol{r})|^2$ is the full condensate density.

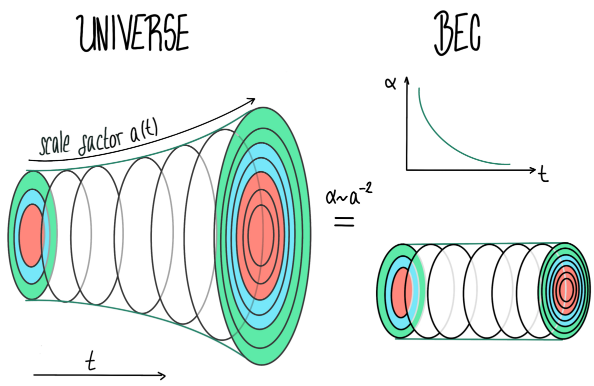

Figure 1. Analogy between BECs and cosmological expansion. Expansion is carried out by decreasing the interaction strength through Feshbach resonance.

This framework can be used to study particle production in the context of inflation through analogs of actions such as

$$S = -\frac{1}{2}\int \mathrm{d}^4x\sqrt{-g}\left[\partial_\mu\varphi\partial^\mu\varphi + \left(m^2 + \xi R\right)\varphi^2\right], \tag{2}$$

which is of interest in early universe cosmology [1, 5]. In this way, analog models of gravity allow for the exploration of the characteristics of quantum fields in curved spacetime straight from the laboratory.

[1] Jose A. R. Cembranos *et al*, *JHEP* ***2020****, 84 (2020).*
[2] Mireia Tolosa-Simeón *et al*, *arXiv:2202.10441 (2022).*
[3] Celia Viermann *et al*, *arXiv:2202.10399 (2022).*
[4] Natalia Sánchez-Kuntz *et al*, *arXiv:2202.10440 (2022).*
[5] Álvaro Parra-López and J. A. R. Cembranos, *in preparation* (2022).

Acknowledgements: Spanish MIU (FPU20/05603) and MICINN (PID2019-107394GB-I00).

Two lines of space reserved to include
codes of the symposium and of this communication

Some uses of dispersion relations

Felipe J. Llanes-Estrada[1]

[1] *Depto. Física Teórica e IPARCOS, Universidad Complutense de Madrid, Spain.*

*e-mail: fllanes@fis.ucm.es

Dispersion relations (pioneered by Kramers and Kronig) are integral identities satisfied by scattering amplitudes. They are a consequence of Titchmarsh's and Cauchy's theorems, and thus of analyticity, that follows from causality in scattering. They cannot be directly derived for partial-wave amplitudes [1] of fixed angular momentum t_J on an object extended to distance R because of an exponential factor $T(s,t,u) \propto \exp\left(-2iR\sqrt{(s-4m^2)}\sin(\theta(s,t)/2)\right)$ diverging when s acquires an imaginary part $+is_I$ in the upper complex plane. Because that factor is $exp(2iR\sqrt{|t|})$, there is no obstacle to derive them for fixed-t amplitudes (also allowing partial waves to satisfy them in certain kinematics). They are extensively used in hadron physics, as I will exemplify for Compton scattering [2] that helped limit the possibilities to solve the proton radius puzzle, or by their use to fix the renormalization scale of the real part of an exclusive amplitude once that of the imaginary part has been chosen [3].

Also useful is the Inverse Amplitude Method (IAM) that leans on applying Cauchy's theorem to an appropriately subtracted inverse amplitude $\frac{1}{t_J(s)}$: the exponential factor now appears in a denominator and becomes a convergence factor.

Dispersion relations do not contain by themselves the full dynamical information of the strong interactions: they are best seen as constraints. However, they become very predictive [5] when combined with the momentum expansion of contemporary Effective Field Theories (EFTs) such as Chiral Perturbation Theory or Higgs Effective Field Theory (HEFT). The IAM is especially well suited to this expansion, because the resulting model amplitude satisfies elastic unitarity *exactly* and allows to exploit the validity of EFTs up to their full range $4\pi f$, whereas they fail, even often near threshold, when the amplitude t_J itself is expanded, because of bad unitarity behaviour. An example of the IAM is shown in figure 1, that shows a resonance predicted from supposed near threshold HEFT parameters that could be measured in the accelerator program. Given this potential use to extend the reach of collider measurements in the electroweak sector, we recently completed an investigation of the uncertainties of the IAM [6].

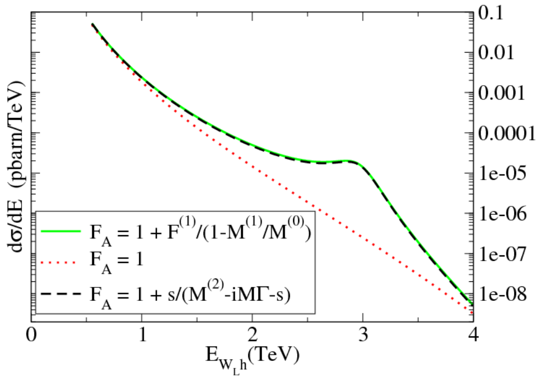

Figura 1: Example $W_L h$ resonance calculated from the IAM as applied to HEFT with coefficients beyond the Standard Model, fed into a form factor parametrization satisfying Watson's final state theorem (thus, having the same pole position as the IAM). (From [4].)

Time permitting, I will describe ongoing work [7] on their use to try to extract the possible slight delay of γ-radiation from astrophysical sources from knowledge of their slight absorption by cosmic electrons (via Compton scattering) or by the Breit-Wheeler process ($\gamma\gamma \to e^- e^+$) on extragalactic background light. Depending on the γ energy, this delay may be measurable by timing events by the arrival of a concurrent gravitational wave and is of interest for multimessenger astrophysics.

[1] F. J. Llanes-Estrada and R. Roldán-González, SciPost Phys. Core **5**, 016 (2022)
[2] M. Gorchtein, F. J. Llanes-Estrada and A. P. Szczepaniak, Phys. Rev. A **87**, 052501 (2013)
[3] S. J. Brodsky and F. J. Llanes-Estrada, Eur. Phys. J. C **46**, 751 (2006)
[4] A. Dobado, F. J. Llanes-Estrada and J. J. Sanz-Cillero, JHEP **03**, 159 (2018)
[5] R. L. Delgado, A. Dobado and F. J. Llanes-Estrada, Phys. Rev. D **91**, 075017 (2015)
[6] A. Salas-Bernárdez, F. J. Llanes-Estrada, J. Escudero-Pedrosa and J. A. Oller, SciPost Phys. **11**, 020 (2021)
[7] D. Beltrán Martínez, F. J. Llanes-Estrada and G. Tejedor García, work in preparation.

Acknowledgements: Supported by grants MICINN: PID2019-108655GB-I00, PID2019-106080GB-C21 (Spain); EU's 824093 (STRONG2020) Univ. Complutense de Madrid under research group 910309 and the IPARCOS institute.

Two lines of space reserved to include
codes of the symposium and of this communication

On the doubly charmed tetraquark T_{cc}^{+} recently discovered at CERN: analysis and predictions

Miguel Albaladejo[1,*]

[1] *Instituto de Física Corpuscular (centro mixto CSIC-UV)*
Institutos de Investigación de Paterna, C/Catedrático José Beltrán
46980 Paterna, Valencia, Spain

*e-mail: Miguel.Albaladejo@ific.uv.es

The neutrons and protons composing the matter that usually surrounds us are made up of three quarks (udd and uud, respectively), which are bound by the so-called strong force. They are a type of particles called *baryons*. But nothing in the underlying theory of strong interactions (called *Quantum Chromodynamics*) prevents the existence of other, more exotic forms of baryons, such as the pentaquarks ($qqqq\bar{q}$). Analogously, most known *mesons* are composed of a $q\bar{q}$ pair, but there can exist also tetraquarks ($q\bar{q}q\bar{q}$). In addition, states can be formed including constituent *gluons* (g), which are the carriers of the strong force, such as hybrid mesons ($q\bar{q}g$) or baryons ($qqqg$), glueballs (gg), etc. Finally, to make it even more interesting, quarks come in six *flavors* (u, d, s, c, b, and t), which generates a humongous zoo of possible particles.

The LHCb collaboration at CERN has recently claimed the discovery of the first doubly charmed meson, named T_{cc}^{+} [1, 2]. Because of the decay properties of this state, we *know* that it is a $cc\bar{u}\bar{d}$ tetraquark. In this talk we report on our recent work [3], in which we have studied the $DD\pi$ spectrum where a prominent signal from the said state is observed, see Fig. 1. We have performed an analysis of the scattering of the $D^{*+}D^0$ and $D^{*0}D^+$ systems, in which the T_{cc}^{+} state should appear. A simple model for the scattering amplitude is used, and it is found to describe well the experimental spectrum. Finally, using Heavy-Quark Spin Symmetry, we predict the location of possible heavier D^*D^* partners.

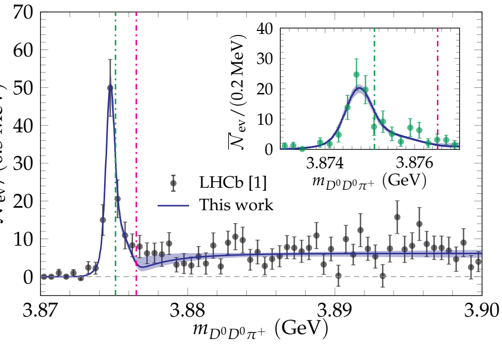

Figura 1: $D^0D^0\pi^+$ spectrum showing the prominent T_{cc}^{+} signal. The data come from the LHCb collaboration [1], and the theoretical curve is our analysis [3]. The green and purple vertical dashed-dotted lines represent the $D^{*+}D^0$ and $D^{*0}D^+$ thresholds, respectively.

Besides the quark content of the state, it is interesting to learn about *how* these quarks are configured inside the state. For the T_{cc}^{+} two possibilities appear, namely a hadron molecule (a loosely bound state of a D^* and a D meson) or a compact tetraquark, in which the four quarks are closely packed and there is no trace of the D^* and D mesons. Using Weinberg's compositeness criterion [4], which is in turn based on simple quantum mechanical arguments, we show that the T_{cc}^{+} state has a large molecular component.

Referencias

[1] R. Aaij et al., LHCb collaboration, *Observation of an exotic narrow doubly charmed tetraquark*, 2109.01038.

[2] R. Aaij et al., LHCb collaboration, *Study of the doubly charmed tetraquark T_{cc}^{+}*, 2109.01056.

[3] M. Albaladejo, *T_{cc}^{+} coupled channel analysis and predictions*, *Phys. Lett. B* **829** (2022) 137052 [2110.02944].

[4] S. Weinberg, *Evidence That the Deuteron Is Not an Elementary Particle*, *Phys. Rev.* **137** (1965) B672.

Two lines of space reserved to include
codes of the symposium and of this communication

Analysis and instrumentation developments for the future understanding of neutrino physics with the T2K experiment

C. Jesús-Valls[1]

[1] *Institut de Física d'Altes Energies (IFAE) - The Barcelona Institute of Science and Technology (BIST), Campus UAB, 08193 Bellaterra (Barcelona), Spain*

*e-mail: cjesus@ifae.es

Nowadays, one of the most active fields of research within high energy physics (HEP) is the study of neutrinos. Despite being theorized in the 1930s and discovered in 1956, neutrinos low interaction probability has slowed down their study notably. It was not until two decades ago that a fundamental property of neutrinos was discovered: neutrino oscillations.

Neutrino oscillations are ruled by six parameters: Three mixing angles ($\theta_{12}, \theta_{13}, \theta_{23}$), two squared neutrino mass differences (Δm^2_{12}, Δm^2_{23}) and one CP-violating phase (δ_{CP}). Concerning their values, three major open questions remain open:

- The θ_{23} octant: Is θ_{23} equal, larger or smaller than 45°?
- The matter-antimatter asymmetry in neutrino oscillations: Is $\delta_{CP} \neq \{0, \pi\}$?
- The mass ordering: Is m_1 larger or smaller than m_3?

A quest has started to answer these questions in what has been named as the era of neutrino precision experiments. Among the existing ones, the Tokai-To-Kamioka (T2K) experiment located in Japan is a leading reference. T2K has been operational since 2010 and has produced some of the most important results in neutrino physics in the last decade: the discovery of a non-null θ_{13}, the best existing constrains for θ_{23} and recently, the first significant hints of a potentially large CP-violation in neutrino oscillations.

Currently, two factors limit further precise measurements in T2K. On one hand, the limited number of collected neutrino events resulting in a significant statistical error. On the other hand, the current systematic errors associated to the event rate predictions. To increase the current statistics, T2K's beam has been recently upgraded and will be upgraded again around 2024, resulting in a 2.6 increase factor of the current neutrino flux. To reduce the systematic errors, two options can be explored:

- Use data to perform dedicated measurements to constrain uncertainties.
- Upgrade the detectors to achieve improved constraints in the future.

My thesis focuses on both of these aspects.

In T2K's oscillation analysis (OA), one of the major nuisances is that of neutrino neutral-current interactions producing a single charged pion in the final state. The current knowledge on this process is very limited, as few tens of events of data have ever been collected in bubble chamber experiments, more than four decades ago. Due to this, constraining this process is crucial in order to alleviate their impact in the OA. In my thesis, using T2K data these interactions are studied in detail for the first time in history.

To measure neutrino interactions, such as the one described above, T2K uses its near detector ND280. ND280 is crucial for the experiment as it constrains the systematic errors associated to the event rate prediction. To push even further the current results of T2K, ND280 is being significantly upgraded with the addition of three new detector technologies: Two new high-angle Time-Projection-Chambers (HATPCs), a novel quasi-3D fully active Super-Fine-Grained-Detector (SuperFGD) and large area plastic scintillator panels which provide very accurate Time-Of-Flight information (ToF panels). In my thesis I have contributed significantly to the development of these new technologies, validating the novel readout of the HATPCs, characterizing and measuring for the first time the PID capabilities of SuperFGD and developing novel Deep Learning reconstruction techniques for SuperFGD and the ToF panels.

With all, T2K is expected to continue to lead the determination of some of the most crucial properties of neutrinos in the next years.

The ATLAS Level-1 Topological Trigger: Run 2 performance and plans for Run 3

Paula Martínez Suárez[1], on behalf of the ATLAS Collaboration
[1] *IFAE-BIST, Universitat Autònoma de Barcelona, Bellaterra (Barcelona), Spain.*
*e-mail: paula.martinez.suarez@cern.ch

The Large Hadron Collider (LHC) is the world's largest particle accelerator. It consists of a 27 km ring with superconducting magnets capable of accelerating protons currently up to 6.5 TeV, thus producing *pp* collisions at a centre-of-mass energy of 13 TeV. The ATLAS experiment [1] is one of the two general-purpose detectors installed in the LHC. It consists of an inner tracking detector surrounded by a thin superconducting solenoid providing a 2 T axial magnetic field, electromagnetic and hadronic calorimeters, and a muon spectrometer. During Run 2 (2015-2018), the LHC delivered *pp* collisions to the ATLAS experiment with an instantaneous luminosity up to 2.1×10^{34} cm^{-2}s^{-1}, at a collision rate of 40 MHz, which is too large to be managed by the detector readout system, storage and offline computing resources. In order to reduce it down to a manageable 1-1.5 kHz while saving as many interesting collisions as possible, the ATLAS detector relies on a two-level trigger system, consisting of a Level-1 trigger (online, hardware) and a High Level trigger (offline, software). The Level-1 trigger is the first rate-reducing step in the ATLAS trigger system with an output rate of up to 100 kHz and a decision latency of less than 2.5 μs, and it provides the input to the High Level trigger.

Since 2017, an important role has been played by the Level-1 Topological Trigger (L1Topo) [2]. This system consists of two AdvancedTCA modules, each of them equipped with two processor FPGAs (Xilinx Virtex7) to run trigger algorithms and one controller FPGA (Kintex7) to communicate with the external trigger systems. Up to 128 algorithms can be implemented to select interesting events by applying kinematic or angular requirements on e/γ and tau clusters, jets, muons and total energy reconstructed in the detector, all of this happening with a latency of 200 ns. This results in a significantly improved background rejection and signal acceptance. The L1Topo system is very important for physics analyses relying on low energy objects, for example Higgs or B-Physics (Fig. 1), where quantities such as the invariant mass or the angular distance between objects are key in order to keep an acceptable trigger rate without the need of raising the energy thresholds.

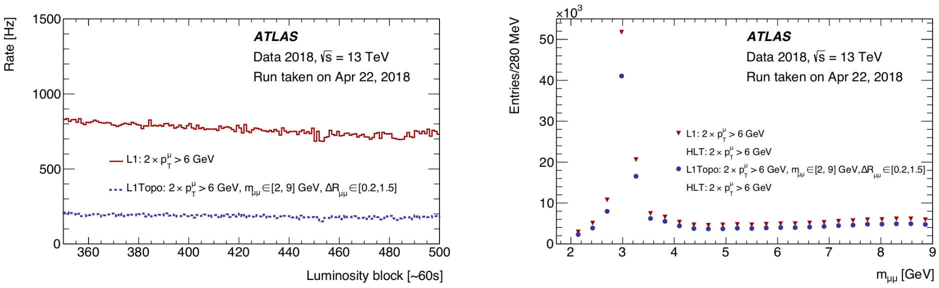

Figure 1. Rate of topological vs. non-topological L1 di-muon triggers w.r.t. time (left) and event acceptance of two HLT triggers seeded by them as a function of the di-muon invariant mass (right). This is an example of how topological requirements can reduce the trigger rates significantly while preserving signal acceptance.

The ATLAS trigger system has undergone several upgrades in preparation for Run 3 (2022-2025), featuring finer granularity in both energy and (η, ϕ) position of the different reconstructed objects, and improved object quality information useful for triggering interesting events. A new L1Topo system with new topological algorithms has been installed and will benefit from all these features. During the beginning of Run 3, the Run 2 L1Topo system will run in parallel for commissioning.

[1] ATLAS Collaboration, *The ATLAS Experiment at the CERN Large Hadron Collider*, JINST 3 (2008) S08003.

[2] ATLAS Collaboration, *Performance of the ATLAS Level-1 topological trigger in Run 2*, CERN-EP-2021-040 (2021).

[3] ATLAS Collaboration,Technical Design Report for the Phase-I Upgrade of the ATLAS TDAQ System, CERN-LHCC-2013-018, ATLAS-TDR-023 (2013).

Two lines of space reserved to include
codes of the symposium and of this communication

Data-Driven Calibration of B-Tagged and Large-R Jets for γ+jet Events in The ATLAS Experiment

Naseem Bouchhar*, Miguel Villaplana, Marcel Vos

Instituto de Física Corpuscular (IFIC), Centro Mixto Universidad de Valencia - CSIC, Valencia, Spain.

*e-mail: naseem.bouchhar@ific.uv.es

The ATLAS detector at the Large Hadron Collider (LHC) consists of four components: The inner detector, EM and hadronic calorimeter and muon detector.

Particles in the LHC often decay hadronically, and these decay products may be reconstructed as jets. Jets are the dominant high-p_T processes in the LHC and play a crucial role in understanding the structure of protons, colour interactions and the coupling strength α_S.

Reconstruction of jets are taken from clusters of topologically connected calorimeter cell signals (called topo-clusters), and from tracks (a charged particle hitting the inner detector) [1].

The energy and mass of jets measured in the ATLAS detector are calibrated via a multi-step process shown in figure 1.

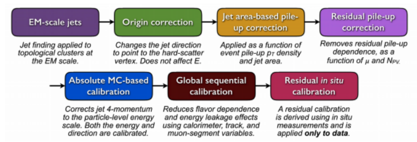

Figure 1. Process for the calibrations of the energy and mass of jets

The focus here is on data-driven (called in-situ) calibration, in which measurements are made in events where the jet recoils against a well-calibrated reference object shown in figure 2. This is to account for discrepancies in the jet response between data and MC.

This talk will be on in-situ calibration results obtained from data-to-MC ratios of the p_T balance between jets and photons for b-tagged jets and large-R jets using the full ATLAS Run2 dataset.

- B-tagged jets: The use of b-tagging is a useful tool in jet analysis that allows one to distinguish from jets originating from the hadronisation of bottom quarks from other quarks. For this talk these jets are small-radius jets (R = 0.4) using Particle Flow Objects (PFOs) [2]. This analysis is using the DL1r tagging algorithm [3].
- Large-R jets: Large-R (R = 1.0) jets clustered with anti-k_t Unified Flow Objects (UFOs), which are a unification of PFOs and TCCs (Track-CaloClusters). [2]

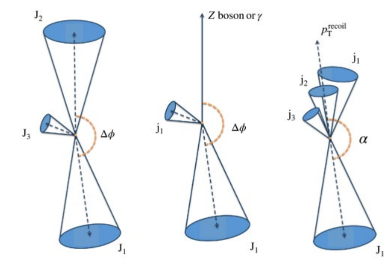

Figure 2. Jet balance against dijet events (left), Z/γ events (middle), multi jet events(right).

[1] The ATLAS Collaboration,Topological cell clustering in the ATLAS calorimeters and its performance in LHC Run 1, *Eur. Phys. J. C* **77**, 490 (2017).

[2] The ATLAS Collaboration, Optimisation of large-radius jet reconstruction for the ATLAS detector in 13 TeV proton-proton collisions, *Eur. Phys. J. C* **81**, 334 (2021).

[3] The ATLAS Collaboration, Optimisation and performance studies of the ATLAS b-tagging algorithms for the 2017-18 LHC Run, *PoS EPS-HEP2017* 733 (2017).

Acknowledgements: We thank CERN for the very successful operation of the LHC, as well as the support staff from our institutions without whom ATLAS could not be operated efficiently. We acknowledge the support of MICINN, Spain and of the GenT Programme Generalitat Valenciana, Spain. And special thanks to Daniel Camarero Muñoz for help in the analysis.

Results of the SDHCAL Beam Test data analysis of 2015

Héctor García Cabrera*, on behalf of the SDHCAL group

Centro de Investigaciones Energéticas, Medioambientales y Tecnológicas.

e-mail: Hector.Garcia2@ciemat.es

The Semi-Digital Hadronic CALorimeter [1] is one of a family of technological prototypes from the CALICE collaboration with the aim to test high granularity technologies for the development of calorimeters in the context of future e^+e^- Higgs Factories. The SDHCAL, built in 2011, is an hadronic calorimeter with Glass Resistive Plate Chambers (GRPC) as active materials and stainless steel as absorber. During the last few years several campaigns of data taking in beam test conditions have been completed, resulting in an analysis of the detector capabilities, energy resolution, development of fine tune corrections and particle identification algorithms.

The data analysis procedures and results are presented. The analysis includes the event building from the raw stream of data into physically meaningful events and algorithms to identify the different particles presen on the beam to create the data sets used for the measurements of efficiency, multiplicity, energy reconstruction and energy resolution. Alongside this measurements, fine tune corrections have been developed to improve and generalize the response of the prototype. These corrections include the study of the incident angle effect and the beam intensity effect.

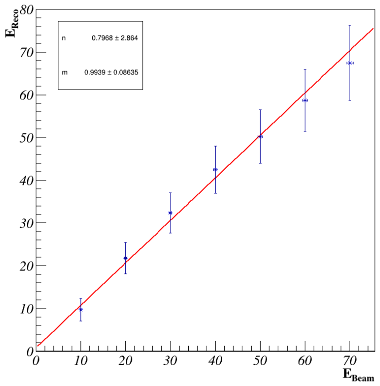

Figure 1. Linearity response of Pions in the SDHCAL

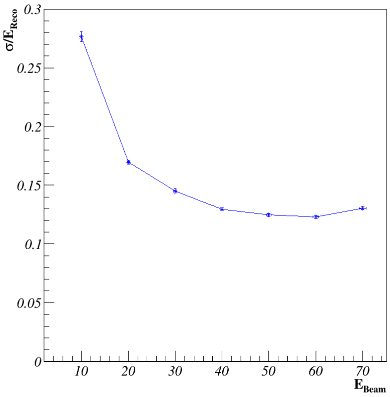

Figure 2. Energy resolution of Pions in the sDHCAL

An efficiency of detection of > 90%, linear response (within +- 10%) and energy resolutions down to 14% have been computed for different angle data sets.

[1] G. Baulieu et al. Construction and commissioning of a technological prototype of a high-granularity semi-digital hadronic calorimeter. *JINST* **10**, P10039 (2015). arXiv: 1506.05316 [physics.ins-det].

IIB orientifold reductions with open strings

Juan R. Balaguer[1], Giuseppe Dibitetto[2,3], Jose J. Fernandez-Melgarejo[4], Alejandro Ruipérez[2,3]

[1] *Departamento de Física, Universidad de Murcia,Campus de Espinardo, E-30100 Murcia, Spain.*
[2] *Dipartimento di Fisica e Astronomia, Università di Padova, via Marzolo 8, 35131 Padova, Italy.*
[3] *INFN, Sezione di Padova, via Marzolo 8, 35131 Padova, Italy.*
[4] *Departamento de Electromagnetismo, Universidad de Murcia,Campus de Espinardo, E-30100 Murcia, Spain.*

*e-mail: juanramon.balaguer@um.es

We consider type IIB compactifications on a general 4D group manifold with different types of possible spacetime filling O-planes and the corresponding D-branes parallell to them. Once fluxes allowed by the associated orientifold projection are included, a 6D $\mathcal{N} = (1, 1)$ gauged supergravity is obtained. We show how the consistent coupling to dynamical open strings living on the spacetime filling D-branes may be captured by the inclusion of extra vector multiplets and extra embedding tensor deformations on the gauged supergravity side. As a result, the quadratic constraints on the embedding tensor consistently reproduce the (modified) 10D Bianchi identities, and the entire scalar potential of the theory exactly matches the one obtained from reduction of the bulk action plus the DBI contributions.

[1] G. Dibitetto, J. J. Fernández-Melgarejo, and M. Nozawa, "6D (1,1) Gauged Supergravities from Orientifold Compactifications," *JHEP* **05** (2020) 015.
[2] E. Bergshoeff, R. Kallosh, T. Ortin, D. Roest, and A. Van Proeyen, "New formulations of D = 10 supersymmetry and D8 - O8 domain walls," *Class. Quant. Grav.* **18** (2001) 3359–3382.
[3] R. C. Myers, "Dielectric branes," *JHEP* **12** (1999) 022.
[4] L. Martucci, J. Rosseel, D. Van den Bleeken, and A. Van Proeyen, "Dirac actions for D-branes on backgrounds with fluxes," *Class. Quant. Grav.* **22** (2005) 2745–2764.
[5] J. Choi, J. J. Fernández-Melgarejo, and S. Sugimoto, "Deformation of $\mathcal{N} = 4$ SYM with varying couplings via fluxes and intersecting branes," *JHEP* **03** (2018) 128.

Acknowledgements: The work of JRB is supported by Fundación Séneca, Agencia de Ciencia y Tecnología de la Región de Murcia, grant 21472/FPI/20.

Two lines of space reserved to include
codes of the symposium and of this communication

Light Detection in DUNE's Vertical Drift Module

Rodrigo Álvarez-Garrote[1], **Sergio Manthey Corchado**[1,*], Laura Pérez-Molina[1] y Andrés de la Torre Rojo [1]

[1] *Departamento de Investigación Básica, CIEMAT, Spain.*

*e-mail: sergio.manthey@ciemat.es

The Deep Underground Neutrino Experiment (DUNE) is an international project at the Long-Baseline Neutrino Facility (LBNF), in the United States. It is hosted by the U.S. Department of Energy's Fermilab laboratory.

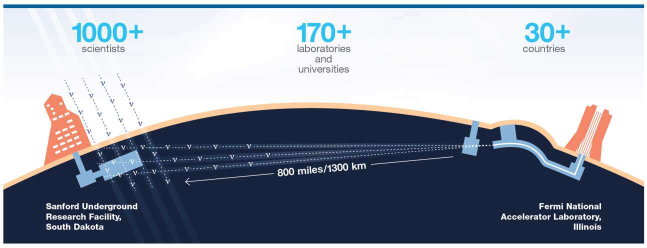

Figure 1. Schematic representation of the DUNE experiment and its different facilities.

DUNE's major goals are to precisely measure the neutrino oscillation parameters, detect neutrinos from supernovas and search for proton decay [1]. It consists of two sets of massive neutrino detectors: Near Detectors (ND) at Fermilab (Illinois) and Far Detectors (FD) 1300 km away at Sanford Underground Research Facility (South Dakota). LBNF produces the world's most intense neutrino beam and provides the infrastructure to study these elusive particles in great detail (Fig. 1).

DUNE's FD will be composed of four Liquid Argon Time Projection Chambers (LAr-TPCs). The proposed configuration for the 2nd FD module is a Single Phase LAr-TPC with electron Drift along the Vertical axis (VD) with two volumes of (13.5 x 6.5 x 60)m^3 dimensions separated by a cathode plane (Fig. 2). The Photon Detection System (PDS) will make use of large size X-ARAPUCA tiles [2] distributed over three detection planes: one horizontal plane with double sided tiles installed on the high voltage cathode and two vertical planes positioned on the longest cryostat membrane walls. The initial performance of the VD PDS using Monte Carlo simulations [3] is currently being estimated.

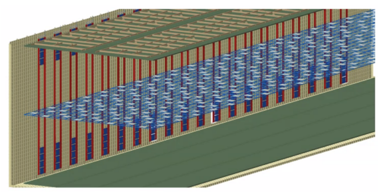

Figure 2. 3D Model of the VD proposal for the 2nd FD module.

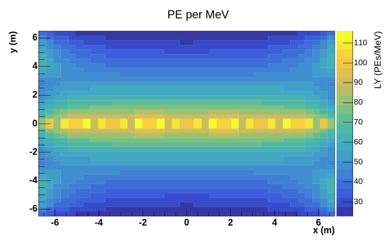

Figure 3. Light-Yield map of the PDS configuration shown in Figure 2.

We present the first studies of the X-ARAPUCA tile distribution over the vertical planes. Different layouts have been simulated in order to optimize the detector's uniformity and maximize the photon collection. Figure 3 shows the number of detected Photo Electrons (PE) per MeV of deposited energy of an example configuration. This information is represented as a Light-Yield 2D map of the central x-y plane (13.5 x 13)m^2 with averaged values over the z axis, being the y axis along the drift direction. These maps have been used to determine which PDS configuration is expected to deliver the best performance.

[1] DUNE Collaboration,*Far Detector Technical Design Report, Volume III*, (2020).

[2] A.A. Machado, E. Segreto, D. Warner, A. Fauth, B. Gelli, R. Máximo, R. A. Pissolatti, L. Paulucci, and F. Marinho, *The X-ARAPUCA: an improvement of the ARAPUCA device*, Journal of Instrumentation, (2018).

[3] L. Paulucci et al, *The DUNE Vertical Drift Photon Detection System*, Journal of Instrumentation, (2021).

Photon Detection System in ProtoDUNE phase II

Rodrigo Álvarez-Garrote[1], Sergio Manthey Corchado[1], **Laura Pérez-Molina**[1,*] y Andrés de la Torre Rojo[1]

[1] *Departamento de Investigación Básica, CIEMAT, Spain.*
*e-mail: Laura.Perez@ciemat.es

The ProtoDUNE experimental program is designed to test and validate the technologies and design that will be applied to the construction of the Deep Underground Neutrino Experiment (DUNE) Far Detector (FD) at the Sanford Underground Research Facility (SURF). The charge detection system permits both calorimetry and position determination. In addition, the photon-detection system (PDS) enhances the detector capabilities for all DUNE physics goals [1].

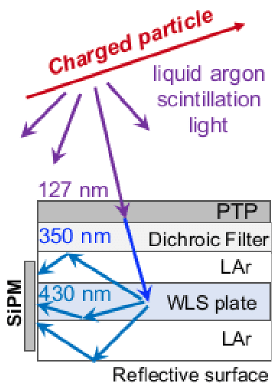

Figure 1. Schematic of the X-Arapuca working principle.

The light collectors, the so-called X-Arapucas [2], are functionally a light trap that captures wavelength-shifted photons inside boxes with highly reflective internal surfaces where they are guided to Silicon Photomultipliers (SiPMs) by wavelength-shifting (WLS) bars.

The two main challenges that the PDS needs to deal with are the difficult detection of the emitted photons ($\lambda \sim 128$ nm) as they are easily absorbed by impurities and the large detection area that is needed.

CIEMAT contribution is focused on the characerization of the X-Arapuca prior to its installation on ProtoDUNE phase II. This final design of the PDS will be installed in DUNE's first FD module.

One of the most important characteristics of the X-Arapuca is its absolute detection efficiency. In order to determine it, we have developed a setup to submerge the X-Arapuca together with reference detectors and an alpha source in Liquid Argon (LAr) at cryogenic temperatures. There are two SiPMs of known efficiency that are used as reference to compute the X-Arapuca one. Also we introduce a Photo-Multiplier Tube (PMT) to monitorize the LAr purity.

The SiPMs and the WLS bar that compose the X-Arapuca are tried in three combinations to see the possible effects on the efficiency. It is computed following two methods so that the results can be cross-checked.

- Baseline method:

$$\epsilon_1(X\text{-}Arapuca) = \frac{PE(X\text{-}Arapuca)}{PE(Ref.\ SiPM)} \cdot \epsilon(Ref.\ SiPM) \cdot f_{corr} \quad . \tag{1}$$

- Simulation method:

$$\epsilon_2(X\text{-}Arapuca) = \frac{PE(X\text{-}Arapuca)}{(LY_{LAr} \cdot En_\alpha \cdot q_\alpha) \cdot f_{sim}} \cdot f'_{corr} \quad . \tag{2}$$

The detected number of Photo Electrons per effective area are indicated as PE. There is a different correction factor depending on the method, but they both correct for the difference in size of the detectors, the SiPMs cross-talk and the fraction of charge not included in the integration range.

The preliminary results obtained with both methods are consistent and so, the X-Arapuca efficiency in LAr is around 2 % for an intermediate SiPM over-voltage. Nevertheless, we are working on improvements for this system, like the the coupling between the bar and the SiPMs, trying to increase the X-Arapuca efficiency for the DUNE FD modules.

[1] DUNE Collaboration, *Deep Underground Neutrino Experiment (DUNE), Far Detector Technical Design Report, Volume III: DUNE Far Detector Technical Coordination*, (2020).
[2] A.A. Machado, E. Segreto, D. Warner, A. Fauth, B. Gelli, R. Máximo, R. A. Pissolatti, L. Paulucci, and F. Marinho, *The X-ARAPUCA: an improvement of the ARAPUCA device*, Journal of Instrumentation, (2018).

Acknowledgements: The work of LPM is supported by the Ministerio de Ciencia e Innovación under FPI contract PRE2020-094863.

Core-Collapse Supernova Burst Neutrino detection and trigger in DUNE

Pablo Barham Alzás[1,*] on behalf of the DUNE Collaboration

[1] *European Organization for Nuclear Research (CERN), 1211 Geneva 23, Switzerland*

*e-mail: pablo.barham@cern.ch

The Deep Underground Neutrino Experiment (DUNE), a next-generation long-baseline neutrino oscillation experiment, will be a powerful tool to perform low energy physics searches including the detection of supernova neutrinos. DUNE will be uniquely sensitive to the electron neutrino flavour component of the burst of neutrinos expected from the next Galactic core-collapse supernova. The experiment will have four modules of 70-kton liquid argon mass in total, placed 1.5 km underground at the Sanford Underground Research Facility in the USA [1].

Core-collapse supernovae are astrophysical events presenting a large source of neutrinos of all flavours. Measuring the neutrino energy spectra, flavour composition and time distribution will be key in understanding the core-collapse mechanism and can provide insights in neutrino physics topics like neutrino absolute masses, mass ordering and exotics like sterile neutrinos or neutrino magnetic moments [2].

In this work we perform a study of the trigger efficiency using the Photon Detection System (PDS) for different detector technologies. We generate a MC sample of supernova neutrino events using the MARLEY event generator [3] and a sample of the most important radiological backgrounds, which are propagated through a full detector simulation. We use a two-step trigger algorithm:

1. We cluster optical hits with certain time and spatial correlations, scanning over a combination of clustering parameters. We select the combination giving us the highest event detection efficiency for a fixed background rate.
2. We compute the trigger efficiency for a range of burst time windows and minimum cluster multiplicities (the minimum number of reconstructed clusters to activate the trigger).

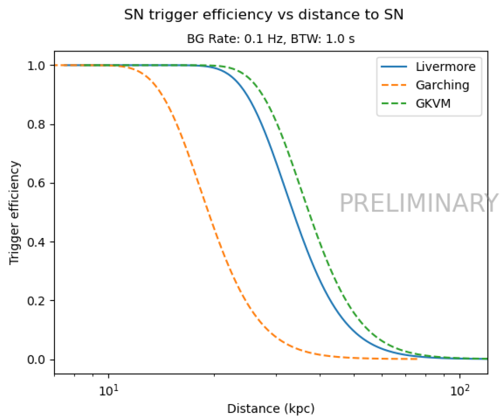

Figure 1. Expected PDS trigger efficiency vs. distance in the Far Detector Vertical Drift module, for three different core-collapse supernova models.

The constraining factor is the tolerated fake trigger rate of 1/month, a DUNE requirement. We find a $\sim 100\,\%$ trigger efficiency up to a distance of over 20 kpc, the distance to the galaxy edge.

[1] DUNE Collaboration, DUNE Far Detector Technical Design Report, Volume III: DUNE far detector technical coordination (2021).
[2] DUNE Collaboration, Supernova neutrino burst detection with the Deep Underground Neutrino Experiment, *Eur. Phys. J. C* **81**:423 (2021).
[3] Steven Gardiner, Simulating low-energy neutrino interactions with MARLEY, *Computer Physics Communications*, **V 269** (2021).